

Crystal Journal of Environmental Science, Innovation & Green Development

Studying the Possibilities of Creating Artificial Clouds and Rain

Abshaev M.T.*, & Abshaev A.M.

Hail Suppression Research Center "Antigrad" 198 Chernyshevsky St. Nalchik Russia 360004

Corresponding Author: Prof. Dr. Magomet T. Abshaev, Hail Suppression Research Center "Antigrad" 198 Chernyshevsky St. Nalchik Russia 360004.

Cite: Abshaev M.T., Abshaev A.M. (2025). Studying the possibilities of creating artificial clouds and rain. Crystal Journal of Environmental Science, Innovation & Green Development, 1(1), 01-23.

Received: July 12, 2025; Accepted: August 05, 2025; Published: August 08, 2025

Abstract

The paper represents results of experimental and theoretical studies of the possibility of creating artificial clouds and precipitation by stimulating convection based on the following physical principles: 1) heating local areas of the atmospheric surface layer using an artificial aerosol layer that absorbs solar radiation; 2) creating an ascending flow jet along a 30-40-tier garland of black screens raised by a balloon and heated by the sun; 3) vertically directed high-speed jet formation maintained by the heat of water vapor condensation on three types of aerosols with different hygroscopic points. The efficiency of these methods was assessed theoretically and in field experiments. It was shown that the use of the first method requires the creation of an optically dense aerosol layer over an area of about 5-10 sq.km that exists for at least 30 minutes. This requires such large dosages of aerosol compositions that the use of this method is expensive and is acceptable due to atmospheric pollution only in desert areas. Verification of the second method showed its complete futility because the large windage of the screens does not allow lifting a garland of more than 4-5 tiers, even in light wind; secondly, adiabatic cooling and wind drift exclude the formation of a continuous updraft by summing the pulses of the ascending flow created by each tier. Field tests of the jet-aerosol method fueled by condensation heat showed the possibility of creating small clouds and local short-term rains. But these results are significantly lower than theoretically expected. The reason for this is that the air humidity on the days with the experiments was below the hygroscopic point of the two types of aerosols introduced into the updraft at the surface level; secondly, the condensation process is not fast enough to provide energy supply to the updraft during its rise, and the power of the D-30 aircraft engine used is insufficient to overcome the surface inversion layers and the destructive effect of the wind. Based on these results, the use of powerful aerospace engines is proposed as a prospect for developing the jet method to create powerful cumulonimbus clouds. The jet of these engines, rising in the atmosphere, can ensure the formation of a powerful convective cloud, into which a novel core/shell hygroscopic aerosol in the required concentration is introduced using a UAV to accelerate the formation of precipitation at an altitude of 400-500 m.

Keywords

Fresh Water Deficit, Desertification, Artificial Clouds and Rains, Convection Stimulation, Hygroscopic Aerosol, Condensation, Jet Stream, Upward Flows, Field Experiments

Introduction

Freshwater scarcity and desertification are one of the global problems of mankind, which is worsening with the growth of the world population, economic development, and climate change. According to the New UNICEF-WHO Report (2023), already about 2.2 billion people do not have access to clean drinking water at home and 3.4 billion people live without basic sanitation. Global population growth by 2050 could increase water demand by 55% and 40% of the world's population will face acute water shortages.

The annual rainfall is about 5.05×1014 m3 of which 1.07×1014 m3 falls on land [1]. There is an average of 715 mm of precipitation per unit area, and about 13,200 m3 (36 m3 per day) of water per inhabitant per year. This is tens of times greater than the demand, but the highly heterogeneous distribution of precipitation across the globe means that some regions are systematically prone to floods and flooding, while other regions with "absolute water scarcity" [2], are experiencing gradual desertification of fertile land.

At latitudes 20° north and south of the equator, almost 50% of precipitation falls, and in some places annual precipitation exceeds 13,000 mm. At the same time, the latitudes from 20° to 35° in the northern and southern hemisphere have the largest deserts, where annual precipitation is 100 mm or less. Global climate warming [3], is degrading and turning into deserts an average of 6 million hectares of fertile land each year, and reducing the productivity of over 20 million hectares. Since 1900, the 4800 km wide Sahara Desert has moved southward by 250 km. As a result, 150 million hectares have been desertified, from which 6 million inhabitants have been forced to emigrate [4]. The Gobi, Libyan, Syrian, Kalahari, Karakum, and other deserts are also expanding. The annual economic damage from desertification amounts to tens of billions of dollars [5].

The drying up of the Aral Sea, 12 lakes with an area of 1,000 to 20,000 km2, and hundreds of smaller lakes has led to the desert-ification and salinization of vast areas in Asia, Africa, Australia, and North America. The causes of this are excessive water extraction for irrigation and urban consumption, overgrazing, deforestation, overpopulation, intensive farming, and climate change.

Land desertification is also observed in the south of the Russian Federation [6], due to excessive grazing and plowing of steppes in hot climates with low rainfall [7]. According to the Russian Academy of Sciences (RAS), 65% of arable land, 28% of hayfields and 50% of pastures in Russia are exposed to erosion, periodic droughts, dry winds, and dust storms [8]. The threat of their desertification forced the Russian Ministry of Agriculture together with the Ministry of Natural Resources and the RAS to establish in 2019. "Center to Combat Desertification of Territories".

In 2019, the UN's "Intergovernmental Panel on Biodiversity and Ecosystem Services" (IPBES of UN) concluded, based on a large-scale study, that "about 75% of the planet's land is significantly degraded and this threatens the security of 3.2 billion people. If this trend continues, more than 90% of land could be unusable by 2050". This means that desertification is a worldwide problem that could lead to a global economic crisis, famine, and population migration.

The traditional sources of fresh water are rivers, lakes, springs, rain, snow and easily accessible groundwater. But their resources are insufficient for domestic needs and the growing demands of agriculture and industry. This is forcing freshwater shortages to be met at an increasing rate by non-traditional sources, including groundwater mining, offshore groundwater extraction, treatment and reuse of municipal wastewater, drainage irrigation and ship ballast water, and finally seawater desalination [9-11]. Despite the abundance of traditional and non-traditional water sources and management solutions to comply with water conservation [12], desertification of territories and expansion of the boundaries of almost all existing deserts continues. Therefore, the search for new sources of fresh water is of high relevance.

The earth's atmosphere contains about 1.3.10¹³ m³ of moisture, of which 98% is water vapor and 2% is clouds [13]. This is 5-6 times more than all the planet's rivers contain [14]. At the same time, atmospheric moisture is an inexhaustible source, as it is

continuously renewed with a periodicity of 40-45 days due to the hydrological cycle of condensation of water vapor \rightarrow precipitation \rightarrow evaporation from the surface of oceans, seas, soil, and plants [15]. Therefore, one of the promising sources of freshwater recharge is the precipitation of part of the atmospheric moisture by using rain enhancement and fogs water harvesting technologies.

The purpose of this paper is to review theoretical and experimental studies of the possibility of creating artificial clouds and rainfall using some new approaches. For this purpose, based on the analysis of the results of previous authors, three different physical principles of creating artificial upward flows and clouds are proposed and tested in the field conditions and a promising variant of developing one of these principles is proposed. The paper contains an introduction, 6 sections and a conclusion. The introduction discusses the relevance of the problem of fresh water scarcity. The first section is devoted to a brief analysis of previously proposed methods and technical means of creating artificial clouds, the second, third and fourth sections are devoted to the theoretical and experimental study of three different physical principles of creating artificial clouds. The fifth section is devoted to the development and discussion of the most promising method for creating artificial rain clouds using the achievements of aerospace techniques, unmanned aviation, and nanotechnology. The main conclusions are summarized in the conclusion.

Previously Proposed Methods for Creating Artificial Clouds and **Precipitation**

One of the ways to replenish freshwater supplies is the application of rain enhancement (RE) methods, which are used in more than 50 countries [16-18]. Traditional RE methods involve enhancing the precipitation efficiency of natural clouds by seeding them with glaciogenic and hygroscopic nuclei using aircraft, rocket, artillery, and ground-based generators. However, in arid regions, the capability of these methods is very limited due to the limited cloud resources. For example, under UAE conditions, with an annual precipitation norm of 80 mm, aerial cloud seeding can increase rainfall by only 5 mm [19, 20].

The question arises whether there is no possibility of increasing the number of days with clouds and increasing the potential for inducing artificial rains, for example, due to situations in which, for example, the development of convective clouds is restrained by the surface layer of inversion or the initial momentum of convection is insufficient. A positive answer to this question is provided by the observed formation of convective clouds in nature over forest and other large natural and artificial fires, active volcanoes, sun-warmed mountain tops, nuclear power plants, thermal power plants, and "heat islands" over megacities. These clouds, called Pyro Clouds and Industry Clouds, are often accompanied by thunderstorms and heavy rainfall even on days when convective clouds are not forecast to develop [21, 22]. Attempts to create such clouds and precipitation have been made since ancient times. Their physical basis is the stimulation of thermal convection by heating localized areas of the surface atmosphere with the help of various heat sources. The oldest method of inducing rain during a drought involved the creation of artificial fires in the prairies and savannahs of South America and Equatorial Africa [23]. In the 1960s and 1970s, there were vigorous attempts to create artificial clouds using meteotrons,

which are thermal sources of warming the surface air generated by petroleum products burning. These include:

- Flare meteotrons tested in France and Cuba [24, 25], which contained 100 or more jet burners placed on an area of 33 m radius. They consumed about 60 and 105 tons/hour of gas oil and had capacities of 700 and 1000 MW. Incomplete combustion of the fuel resulted in heavy soot pollution, but could also warm the jet by absorbing solar radiation.
- Flamethrower meteotron of the Institute of Geology and Geophysics of the Siberian Branch of the Russian Academy of Sciences [26], which had 60 jet flamethrowers placed on the perimeter of an octagon with a side of 53 meters. It developed a power of 5-6 GW and consumed about 430 tons/hour of diesel fuel. Rising streams containing black smoke rose to heights of up to 3 km in some of the 8 experiments.
- Meteotrons of the Chelyabinsk Polytechnic Institute (8 variants), were designed to ventilate coal mines, create clouds and disperse fog. They contained from 10 to 100 centrifugal nozzles with diesel fuel consumption from 7 to 30 tons/hour, and developed power from 80 to 400 MW [27, 28]. Fine atomization of diesel fuel in combination with different nozzle placement options ensured complete combustion of fuel and smokeless jet.
- Meteotrons of the Institute of Applied Geophysics of the USSR Hydromet with 4 and 10 jet engines, designed to investigate the possibility of creating artificial clouds and precipitation, had capacities of 200 and 500 MW, and the "Super Meteotron", built on the shore of the high mountainous Lake Sevan to replenish its water level, contained 6 engines with a total capacity of 500 MW [26]. On the basis of theoretical modeling of jet rise, it was shown [26, 29], that at a meteotron power of about 103 MW, the upward jet could reach a height of 600-1000 meters. In some experiments, under favorable conditions, the formation of small convective clouds or intensification of existing clouds was noted.
- A device for initiating an annular vortex of air using 50-60 aircraft engines arranged in a ring with a radius of 800 m and numerous seawater atomizers inside and outside the ring [30].
- Proposals to stimulate the development of artificial clouds and precipitation by heating the surface air layer with solar meteotrons are also known:
- The simplest solar meteotron is a patch of ground surface covered with asphalt, black cloth, or vegetation that absorbs solar radiation well and can create "heat islands" [31-33].
- Blackened screen elevated above the ground and surrounded by a system of rotating mirrors focusing solar energy onto the screen [34].
- A method of changing the albedo of the underlying surface by means of green plantings or covering with solar panels [35, 36]. Brenig et al. found that the air above a surface with low albedo, is heated more by sunlight, rises upwards and leads to a rise in sea breeze. This promotes cloud development and increased rainfall on the leeward side 25-30 km inland.

None of these methods is not applied in practice and all of them are still the subject of research and separate experiments, as the ancient method of burning prairie vegetation and shrouds is not acceptable due to the inadmissibility of burning bioresources and harm to flora and fauna, flare and flamethrower meteotrons have proved to be ineffective, small solar meteotrons are not effective, and large ones are not created, also the device with 50-60 aircraft engines and hundreds of water sprayers is not realized.

Within the framework of project No. APP-REP-2017-02120 [37], we investigated the possibilities of stimulating convection and creating artificial clouds based on the following three updated approaches:

- heating of localized regions of the surface atmosphere from solar radiation by creating an artificial aerosol layer consisting of finely dispersed aerosol that effectively absorbs solar radiation:
- heating a vertical column of air from solar radiation by means of a multi-tiered Heliator device having a garland of black fabric cones lifted by helium-inflated balloons;
- creation of artificial updraft by means of vertically directed high-temperature buoyancy jet saturated with hygroscopic aerosol with the purpose of jet energetic feeding by heat of water vapor condensation.

Aerosol Layer as a Solar Meteotron

This method involves the creation of artificial clouds, similar to Pyro-Clouds formed in nature over large forest and other large fires [21, 31, 38], and Industry-Clouds formed over heat islands arising over megacities [39-42], nuclear and thermal power plants [43]. For this purpose, it is proposed to create an artificial aerosol layer that absorbs solar radiation well, warms the surface air, initiates thermal convection and convective cloud formation [44-46]. Creating such a solar meteotron is much easier and cheaper than covering with asphalt or black cloth areas commensurate with large forest fires, volcano craters, or urban heat islands over which Pyro Clouds are formed.

To verify the performance of this method, the following tasks were accomplished: selection of the optimal aerosol dispersity, design, fabrication and testing of smoke compositions generating an aerosol that effectively absorbs solar radiation, settles slowly and has hygroscopic properties; modeling of the aerosol diffusion process from discrete and continuous sources due to turbulent diffusion and wind transport; design and fabrication of smoke checkers and field experiments to create an aerosol layer.

Chosen of the Aerosol Dispersity was so that the absorption maximum was in the wavelength band from 0.3 to 0.9 μ m, where the main solar radiation flux is concentrated. Calculations of the absorption coefficient of solar radiation in the aerosol layer were carried out on the basis of the theory of electromagnetic wave scattering using the formula:

$$\gamma(\lambda, m, r) = \int_{0}^{\infty} n(r) \, \sigma_{\rm a}(\lambda, m, r) \, dr \, (2.1)$$

where r is the radius of aerosol particles; λ is the wavelength; n(r) is the size distribution function of aerosol particles; $\sigma_a(\lambda, m, r)$ is the absorption cross section of aerosol particles calculated by exact diffraction formulas [71]; $m = n-i\kappa$, is the complex refractive index of the particle substance, where n is the refractive index and κ is the absorption index; $n = 0.047\lambda + 1.4317$; $\kappa = -0.008\lambda + 0.756$.

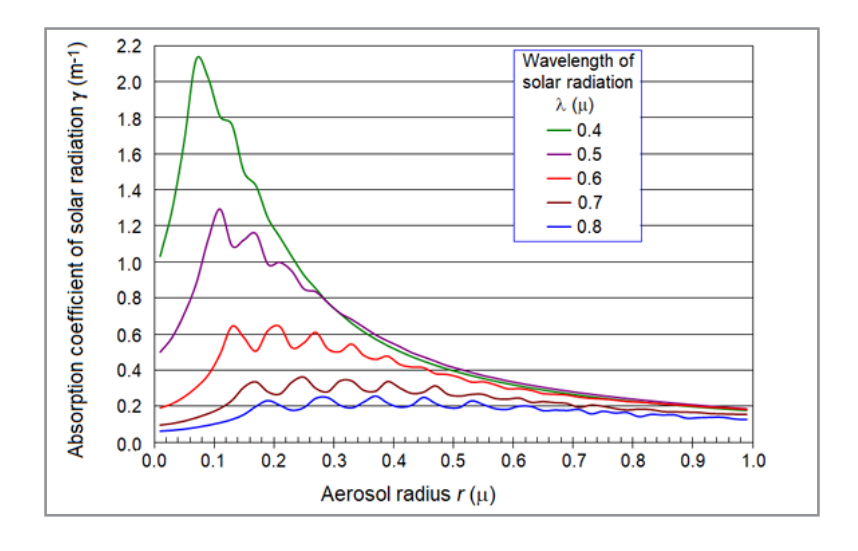


Figure 1: Absorption coefficient of solar radiation (γ , m⁻¹) at dose of aerosol composition 0,25 g.m⁻² depending on the radius of aerosol r.

Calculations have shown that the value $\gamma(\lambda.m.r)$ in the wavelength range $0.4 < \lambda < 0.8 \, \mu m$ has a maximum at aerosol radius from $0.05 < r < 0.2 \, \mu m$, having also negligibly small gravitational settling velocity. At aerosol dispersity $r = 0.1 \, \mu m$ with 1 gram of smoke composition, about N $\approx 1.2 \times 1014$ particles having a density of 2 g.cm⁻³ come out. It follows from figure 1 that at the dosage of the smoke composition about $0.25 \, g.m^{-2}$, or the number of particles per unit area NAS $\geq 3 \times 10^{13} \, m^{-2}$, almost complete absorption of solar radiation in the visible wavelength range is provided.

The Study of Aerosol Propagation due to turbulent diffusion and wind transport was carried out on the basis of numerical solution of Eq:

$$\frac{\partial N}{\partial t} + u \frac{\partial N}{\partial x} + \left(w - V_g\right) \frac{\partial N}{\partial z} = D_T \left(\frac{\partial^2 N}{\partial x^2} + \frac{\partial^2 N}{\partial y^2} + \frac{\partial^2 N}{\partial z^2}\right),\tag{2.2}$$

where is the volumetric concentration of aerosol particles; u and w are horizontal and vertical wind speeds; $V_g = \int_0^\infty \omega(r) r^3 N(r) dr / \int_0^\infty r^3 N(r) dr$ is the aerosol gravitational settling velocity; $\omega(r) = 2g(\rho - \rho_0) r^2 / 9\eta$ - sedimentation velocity of a particle of radius r; ρ and ρ_0 - density of aerosol particle and air, respectively; η - dynamic viscosity of air; DT - turbulent diffusion coefficient.

For the numerical solution of equation (2.2), the origin of coordinates is placed at the point of aerosol emission, the X-axis is directed along the wind direction, and the Z-axis is vertically upward. The condition of complete absorption of aerosol particles is set at the ground surface, and the condition of complete reflection is set at the upper boundary, leading to the accumulation of impurity in this layer.

At the initial time instant, the aerosol particle concentration distribution for an instantaneous point source is given in the form:

$$N(x, y, z, t_0) = \frac{N_{01}}{D_T (2\pi\sigma^2)^{3/2}} \cdot exp\left\{-\frac{1}{2\sigma^2} [(x - x_0)^2 + (y - y_0)^2 + (z - z_0)^2]\right\},$$
(2.3)

where N01 is the number of instantaneously generated particles; - the mean square of the initial distances between particles, determined by the initial size of the aerosol cloud; - the point of aerosol introduction.

In the case of a continuous point source, the particle number replenishment is given in the form:

$$N(x, y, z, t) = N(x, y, z, t_0) + \frac{N_{02}}{D_T (2\pi\sigma^2)^{3/2}} \cdot exp \left\{ -\frac{1}{2\sigma^2} [(x - x_0)^2 + (y - y_0)^2 + (z - z_0)^2] \right\},$$
(2.4)

where N_{02} is the number of particles produced by the source per unit time

According to such modeling data, five continuous sources spaced 200 m apart across the wind direction, burning 100 kg of smoke composition for 1 hour each, can produce a continuous aerosol layer with a particle number in the vertical column NAS > 1013 m-2 over an area of about 1.5 km2 at a wind speed of 0.5 m.s⁻¹ and over 3 km2 at a wind speed of 1 m.s⁻¹.

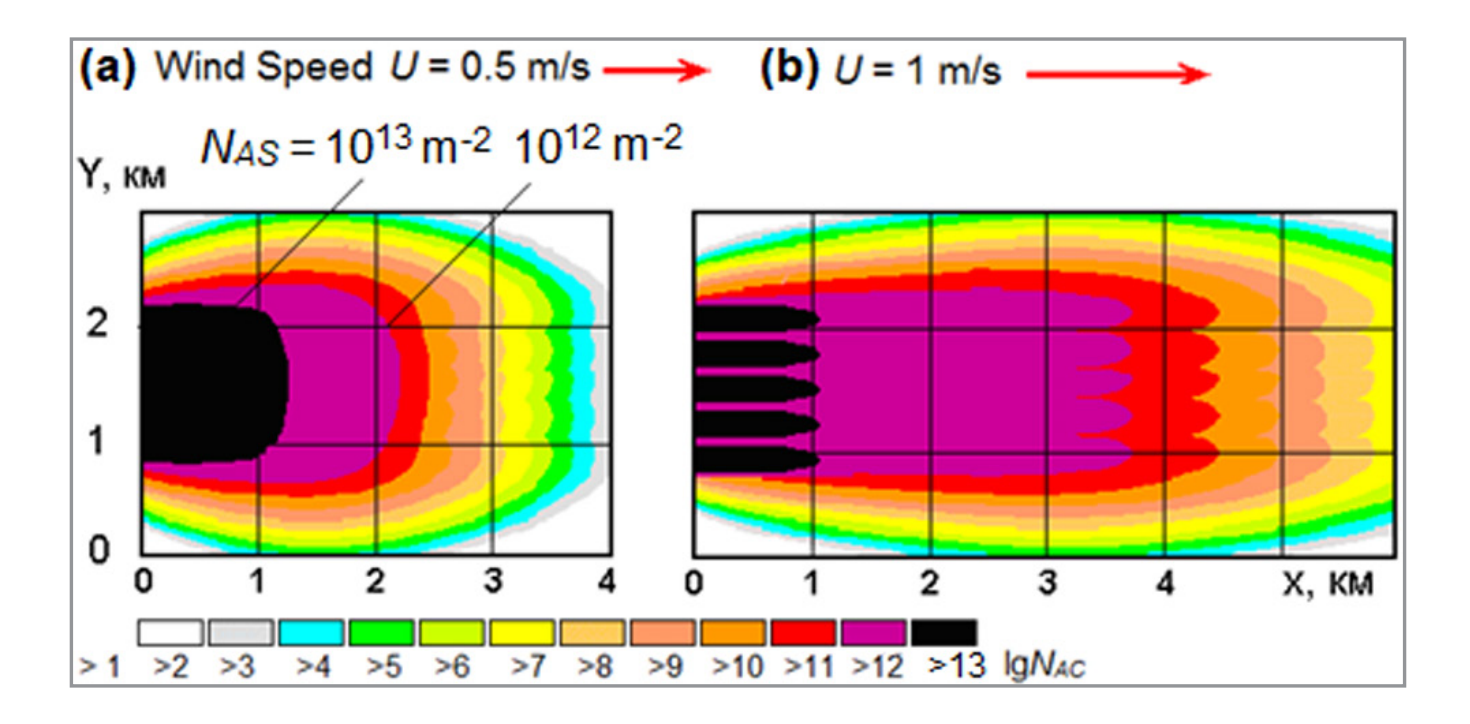


Figure 2: Aerosol concentration field created after 1 hour of continuous operation of 5 sources, located at 200 m intervals across the wind at a total aerosol composition flow rate of 500 kg: a) at wind speed U = 0.5 m.s⁻¹; (b) at wind speed U = 1 m.s⁻¹.

(2.5)

The Amount of Solar Radiation Energy Absorbed by the Aerosol Layer, which leads to the formation of a heat island, was estimated using the formula:

$$Q = P(\lambda) \cdot \Delta \lambda \cdot \gamma \cdot S \cdot \sin \theta \cdot (1 - A) \cdot t,$$

where $P(\lambda)$ is the spectral radiation density of the Sun; λ is the wavelength; $\Delta\lambda$ is the width of the absorption band of the aerosol layer; γ is the absorption coefficient of solar radiation; S is the area of the aerosol layer; θ is the angular position of the Sun; A is the albedo of the landscape surrounding the aerosol layer; t is the duration of the aerosol layer.

Assuming that at the surface of the earth P (λ) = 1 W.(M^2 .nm)⁻¹, $\Delta\lambda$ = 600 nm; γ = 0.9 m⁻¹; aerosol layer area S = 2×10⁶ m²; θ = 70°; albedo of the environment (e.g., for a desert) A = 0.35; t = 0.1 hour, we obtain that the amount of heat absorbed by the aerosol layer is Q = 6.6×10⁴ kWh = 2.4×10⁸ kJ. This heat goes to heat the air in the aerosol layer and can cause its temperature to rise above its surroundings by ΔT equal to:

$$\Delta T = \frac{Q \cdot t}{M_a c_p} = \frac{Q \cdot t}{S \cdot h \cdot \rho_0 \cdot c_p} = 3.6 \,^{\circ}\text{C}$$
 (2.6)

where cp = 1.005 kJ.(kg °C)-1 is the heat capacity of air at constant pressure, and Ma is the mass of heated air; h is the thickness of the aerosol layer; ρ_0 is the air density.

At S = 2×10^6 m², h = 30 m, air density at the height of the experiments (1000 m above sea level) ρ_0 = 1.11 kg.m⁻³ the mass of heated air will be Ma = 6.7×10^7 kg. In 6 minutes after creation of the aerosol layer, the air temperature excess in it can reach ΔT = 3.6 oC. Such an excess of air temperature in the aerosol layer relative to the surroundings will inevitably lead to forced rise of heated air and development of convection. Continuous operation of the aerosol source can lead to the increase in time of the area and volume of the upward flow up to the volume comparable to that of Cu Cong even without considering the involvement of ambient air.

Numerical Modeling of Convection Stimulated by an Aerosol Layer was carried out based on the solution of the system of Navier-Stokes equations within the framework of the computational fluid dynamics (CFD) package suite FlowVision [47, 48]. Figure 3 shows the simulation results of upward flow velocity fields that can initiate aerosol layers in a windless atmosphere having areas of S1 = 104, S2 = 105, S3 = 106, and S4 = 107 m2, respectively. As would be expected, the lift height and volume of the initiated upward flow increase as the area of the aerosol layer increases.

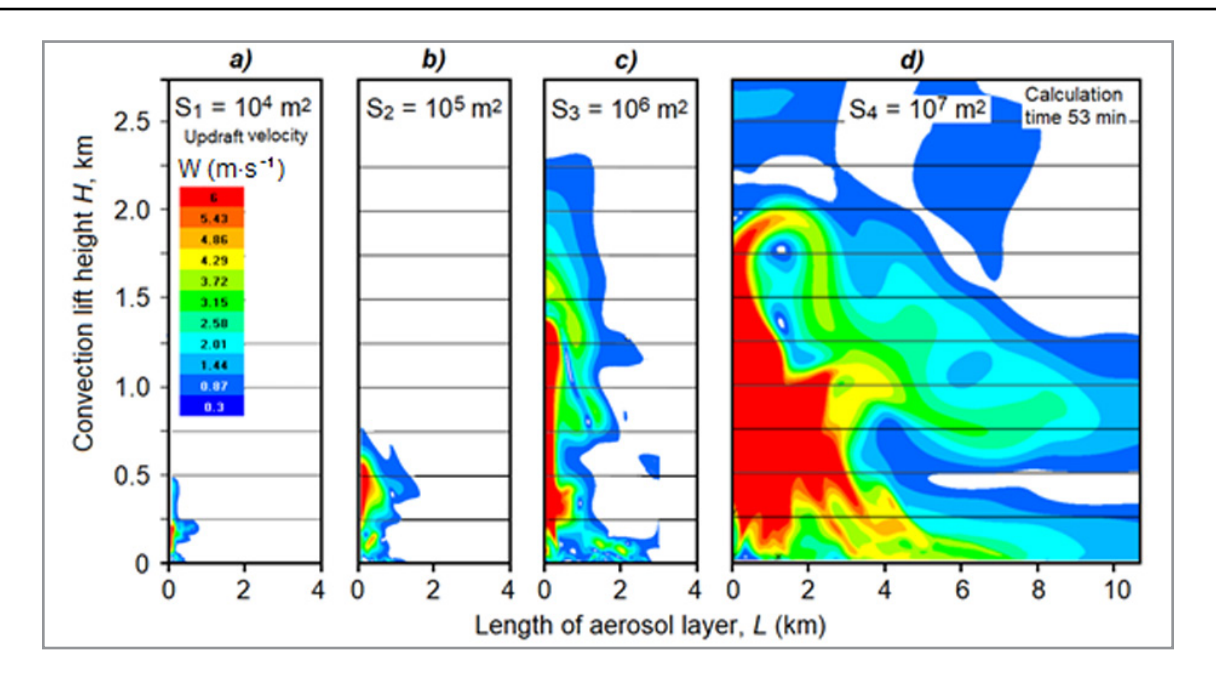


Figure 3: Rise height and velocity of the updraft caused by the action of an artificial aerosol layer having an area of 10^4 , 10^5 , 10^6 , and 10^7 M^2 .

An aerosol layer with an area of 5-10 km2 has a high probability of initiating thermal convection and the development of artificial convective clouds in a windless atmosphere and at low wind speeds. This probability may decrease sharply with increasing wind speed and wind shear, as can be seen in Figure 4b.

Aerosol Compositions and Checkers. For practical realization of the aerosol method 6 variants of smoke compositions generating aerosol of optimal size for solar radiation absorption were developed. To test these compositions, ACH-1 checkers of 26 mm caliber and 10 g mass of smoke composition were manufactured Fig. 4). Laboratory tests of these checkers were carried out in cloud chambers by combustion in a horizontal wind tunnel at a blowing speed of 2 m.s⁻¹, with sampling and measurement of the particle spectrum in a 12 m3 cloud chamber. The aerosol spectra of the four compositions obtained with Laser Aerosol Spectrometer 3340 and Electrostatic Classifiers TSI 3080 analyzers are presented in Figure 4a.

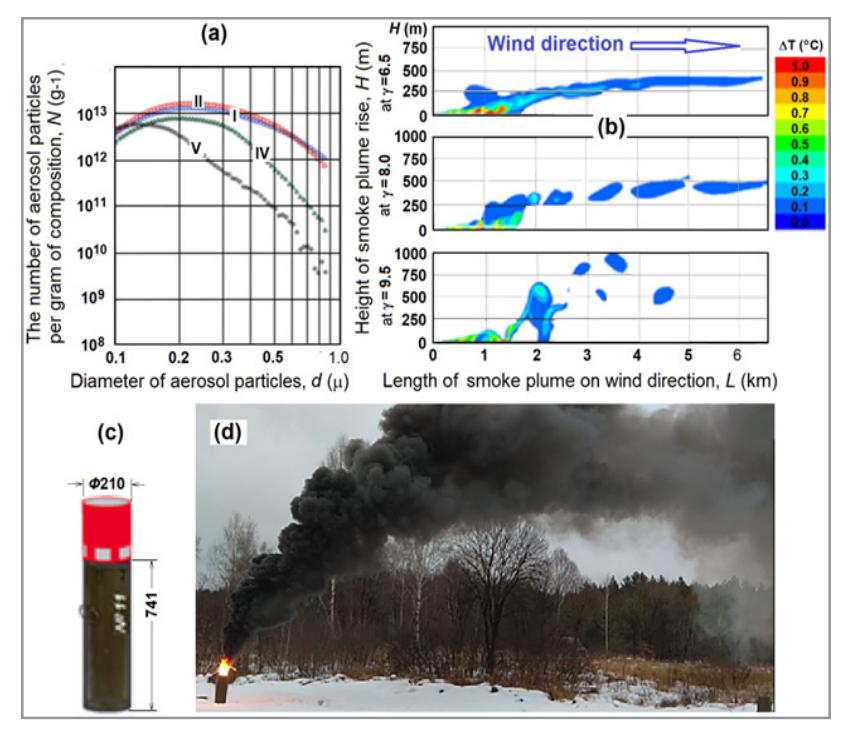


Figure 4: Aerosol compositions and checkers: (a) aerosol spectrum generated by smoke compositions number I, II, IV, and V; (b) – CFD simulated temperature field of aerosol plumes generated by continuous aerosol source for 20 min at wind speed U = 1 + 0.05H (m.s⁻¹) and different atmospheric temperature lapse rates $\gamma = 6.5$, 8.0 and 9.5 °C.km-1; (c) – ACH-1 aerosol checker with injector (red color); (d) – real aerosol plume in field tests.

On the basis of tests of optical properties of generated aerosols, 2 most effective compositions creating aerosol with a median diameter of 0.21 and 0.22 microns were selected and 10 pieces of aerosol smoke bombs ACH-1 and ACH-2 were manufactured each. These bombs had a metal case in the form of a cylinder with a diameter of 210 mm, height of 741 mm (figure 4c) and a remote electric ignition device. The mass of the smoke composition in each checker was 25-30 kg. The aerosol yield from one gram of the I and II versions of the smoke composition was 4.6×1013 and 5.6×1013 . Consequently, one checker generated about 2.5×1018 aerosol particles.

Field Tests of Aerosol Checkers were conducted at the experimental site from October 02 to November 12, 2019 under rather harsh conditions when the gusty wind speed reached 3-7 m.s⁻¹. Aerosol clouds in these conditions rose to a height of several hundred meters and were pulled downwind (figure 4d). The burning time of the checkers was about 9.3 minutes, the area of the aerosol layer created by one checker was about 3000-4000 m2, the dissipation time of the aerosol cloud after the end of the checker burning was 3-5 minutes.

The aerosol practically did not settle due to small size, but under the action of gusty wind its concentration quickly decreased and the smoke plume became invisible. Based on the field tests results, it follows that to create an aerosol layer with the required optical density over an area of 5 km2 and to maintain the concentration of particles about NAS $\geq 3 \times 1013$ m-2 for 30 minutes requires about 400 smoke checkers of ACH-1 or ACH-2 type with a total mass of aerosol composition of 10 tons. Under more gentle atmospheric conditions (with wind speeds of 1-2 m.s⁻¹ and no wind gusts), this consumption can be reduced by a factor of two or more. In order to reduce this consumption, two more variants of the aerosol composition were developed and 2 checkers were manufactured, which generate a finer aerosol with a modal diameter of 0.03 µm and a yield from 1 gram of composition of about 4.4×1015 particles (at least 1020 particles from one checker). To create the required optical density, the aerosol concentration of this size per unit area must be at least NAS ≥ 6×1013 m-2. Thus, to create a 30-minute aerosol layer on the area of 5 km2 about 70 a checkers will be required.

Instead of smoke checkers aerosol generators of TDA-2K type can be used, which can work 2- 3 hours on one refueling and create an aerosol layer over large areas. In any case, to stimulate convection and development of artificial clouds it is necessary to create an aerosol layer with sizes comparable to the sizes of large fires and heat islands over megacities, over which Pyro and Industry clouds are formed. And this requires large expenditures of smoke compositions. Therefore, despite the ecological purity of the developed smoke compositions, this method can be used only in sparsely populated desert areas for environmental safety. The estimates presented here may be useful for understanding the effects of burning oil puddles, aerosol emissions from volcanoes and the conditions of Pyro and Industry clouds formation.

Multitier Garland of Black Screens

This method involves the Heliator-2 device, which is a 30-40 tiers garland of black screens of toroidal shape with a diameter of 15 m, lifted by a helium-filled balloon (figure 5a).

It was assumed that each black screen would be heated by the Sun, warming the adjacent air and initiating an updraft reaching the next tier. Repeating this process on all tiers could result in the formation of an updraft jet reaching the height of the condensation level and the formation of an artificial cloud (figure 5c). In order to enhance the effect, the Heliator-2 device should be raised above an aerosol layer or a blackened circle that absorbs solar radiation, and spark ionizers should be installed on each tier so that the ions formed contribute to the condensation of water vapor [49].

Field tests of the prototype Heliator-2 device, showed that the high sailing of the screens does not allow to lift the garland having more than 4-5 tiers even in low wind (figure 5b). CFD simulations on a supercomputer using ANSYS and FlowVision packages showed that adiabatic cooling and wind drift complicates the overcoming of heated air by the height difference between the tiers and the formation of a continuous updraft jet, and at wind speeds greater than 1 m.s⁻¹ wind drift excludes the addition of upward flows created by each tier (Figure 5d). Thus, experimental and theoretical studies have shown that this principle of creating artificial clouds is not promising.

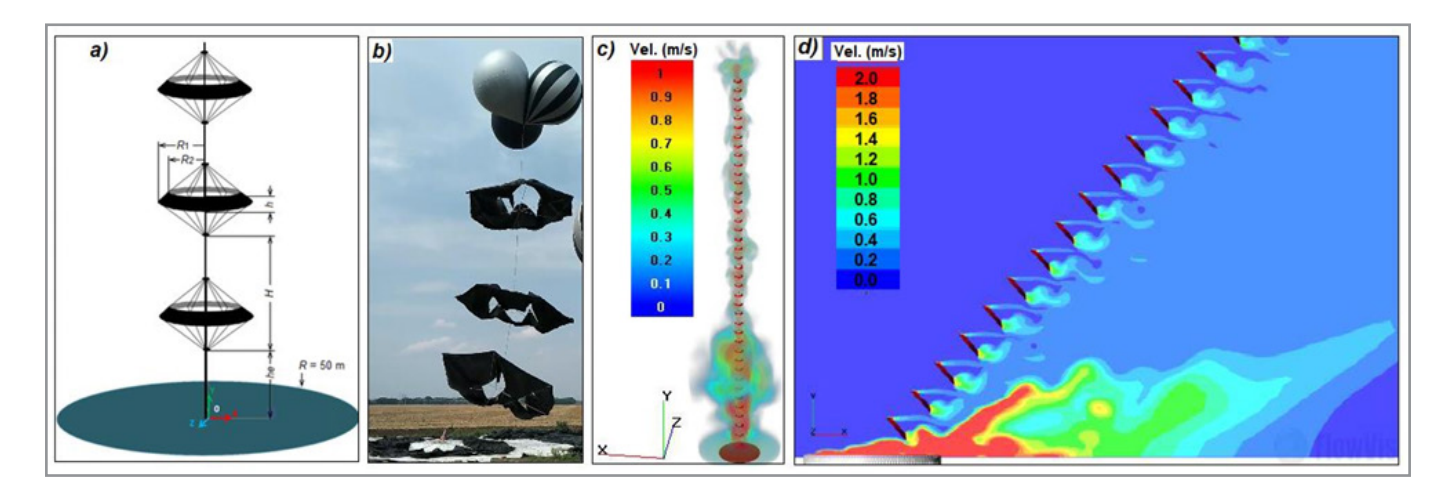


Figure 5: Multitier device Heliator-2: (a) Design of Heliator-2; (b) Experimental prototype of Heliator 2 in real atmosphere; (c) Simulated updrafts velocity in a windless atmosphere; (d) Tilting of thermal bubbles generated by Heliator-2 in a windy atmosphere. It can be seen that the wind tilts the garland of screens and blows down the updrafts stimulated by each tier excluding the summation of the effects of a multi-tiered system.

Jet Method

Physical Basis of the Method

This method involves the creation of artificial clouds using a vertically directed buoyancy jet initiated by an aircraft engine. Its fundamental difference from the previously proposed meteotrons [26], is that the jet is saturated with three types of hygroscopic aerosol near the surface level in order to energetically feed the jet with the heat of water vapor condensation on these aerosols [50].

To improve energetic recharge, hygroscopic substances with different hygroscopic points are used. The first of them CaCl2 is a very strongly hygroscopic substance with hygroscopic point RH1<6%, the second (NH2)2CO is another strongly hygroscopic substance with hygroscopic point RH2 = 66.5%, and the third is a substance NaCl with hygroscopic point RH3 = 78% [74]. All three types of aerosols were introduced into the jet by spraying concentrated aqueous solutions using a system of nozzles placed along the contour of the jet or powerful fogging guns spraying from 0.6 to 1.0 L of solution per minute. Solutions of all substances were sprayed to droplets of about 15 µm diameter so that their evaporation formed aerosols of $10 \pm 3 \ \mu m$ diameter at a concentration of about $(4-5)\times 1011$ particles of each type per second. It was assumed [51], that these three types of aerosols would provide intensive condensation of water vapor, release of condensation heat, and enhancement of the updraft velocity and height of its ascent at air humidity from 6% to 78% throughout the sub cloud layer to the level of natural cloud formation.

In addition to the above three substances, NaCl/TiO2 nano-powder [52, 53], which can condense many times more water vapor than the listed aerosol types, was also used in the field experiments.

Estimating the Heat of Condensation

Hygroscopic aerosol provides condensation of water vapor at densities lower than the saturating density, thereby lowering the height of artificial cloud formation. It was shown in [51], that the maximum amount of water vapor mw that can be condensed by an aerosol particle of mass ma can be estimated using the formula:

$$m_w = m_a \left[(1 + \kappa) \frac{c_c}{c_s} - 1 \right], \tag{4.1}$$

where κ is the ratio of the mass of condensed water to the mass of dissolved matter in the saturated solution; CC = ES/E is the ratio of the water vapor pressure over a drop of saturated solution ES to the pressure over a flat surface of distilled water E; CS = $\Delta ES/E\infty$ is the ratio of the difference between the indicated pressures ΔES to the vapor pressure in the environment $E\infty$. The values of κ , CC, and CS are given in reference books [54].

Table 1 shows the amount of each type of solute introduced into the jet stream every second during the experiments, the number of aerosol particles N formed, the particle condensation growth coefficient k1, the mass of water condensed on one particle mw, the mass of water condensed on all particles Mw, and the maximum amount of latent heat of condensation PC that could be released.

Table 1: Flow rate of hygroscopic substances introduced into the jet during in-situ experiments, expected amount of water vapor and released heat of condensation.

Hygroscopic Substance	Substance mass flow rate M (g×s-1)	Aerosol flow rate N (Pcs. ×s-1)	Growth f actor k1 = md/ma	Water vapor mass con- densed on one particle, mw = k1×ma (g)		
NaCl	215	1.90×1011	5.86	6.62×10-9	1.26	2.85
CaCl2	538	4.78×1011	1.67	1.87×10-9	0.9	2.03
(NH2)2CO	672	5.32×1011	3.08	2.15×10-9	2.07	4.75
*NaCl/TiO2	230	1.62×1012	19.4	2.74×10-9	4.46	10.08
**CaCl2	476	3.38×109	1.67	2.35×10-7	0.79	1.79

Note: NaCl/TiO2 and CaCl2 was applied in the form of powders with particle sizes of about 5 m and 50 m.

When the experimental setup is operated using three substances (NaCl, CaCl2 and (NH2)2CO) in the quantities shown in the first three rows of Table 1, at an air humidity of RH > 80%, 4.23 kg of water vapor can condense every second with a condensation heat release equal to:

$$Pc = \Sigma M_{wi} \times q = 4.23 \text{ kg} \cdot \text{s}^{-1} \times 2260 \text{ kJ} \cdot \text{kg}^{-1} \approx 9.6 \text{ MJ s}^{-1} = 9.6 \text{ MW s}^{-1}.$$
 (4.2)

This is equivalent to making the jet power of a D-30 aircraft engine equal to 69 MW increase by almost 14%. Introducing 476 g s-1 of NaCl/TiO2 aerosol into the jet stream at an air humidity RH > 66.2% can result in condensation of 4.46 kg s-1 of water and release of condensation heat of about 10.08 MJ s-1. This amount of heat can appreciably increase the energy of the jet, especially at the stage when its temperature equalizes with the ambient air temperature and it loses buoyancy.

Numerical Modeling of Jet Motion in the Atmosphere

To investigate the possibility of creating artificial clouds and precipitation by means of a vertically directed jet saturated with hygroscopic aerosol, 3-D modeling of the jet motion in the atmosphere with and without feeding by water vapor condensation heat was carried out. On the basis of the CFD FlowVision software package suite, a geometric 3D model was created in which the computational domain was divided into two parts: the lower part, where the high-speed jet exits the nozzle, and the second part, where the jet moves in the free atmosphere [47]. This separation is necessary for a more correct calculation of the turbulent jet motion having an initial near-sonic velocity (M > 0.3), taking into account the compressibility of the gas and the need for a high resolution of the computational grid of the jet velocity and temperature fields. The calculations in the second part were car-

ried out using the large-scale atmospheric flow model, where the system of thermal convection equations in the Boussinesq approximation, including the Navier-Stokes, heat conduction and incompressibility equations, was numerically solved using the incompressible formulation. The description of the model, the system of equations and the solution method is given in Abshaev and Aksenov et al., 2022b. The height of the entire computational domain, including the initial and subsequent section, is $2-6 \, \mathrm{km}$, the length of the computational domain along the main wind direction is 6 km. Each computational case is solved in a full 3D representation, as it is necessary due to the presence of

dependence of the velocity vector direction on height. Numerical experiments to calculate the structure of the jet velocity and temperature fields and the concentration of aerosol injected into the jet revealed the following patterns:

The motion of a high-temperature jet in the real atmosphere has a complex turbulent character due to its high initial velocity. The vertical velocity and temperature fields of the jet, as well as the aerosol concentration, are highly inhomogeneous and pulsate around the jet axis even in a windless atmosphere (see figure 6b).

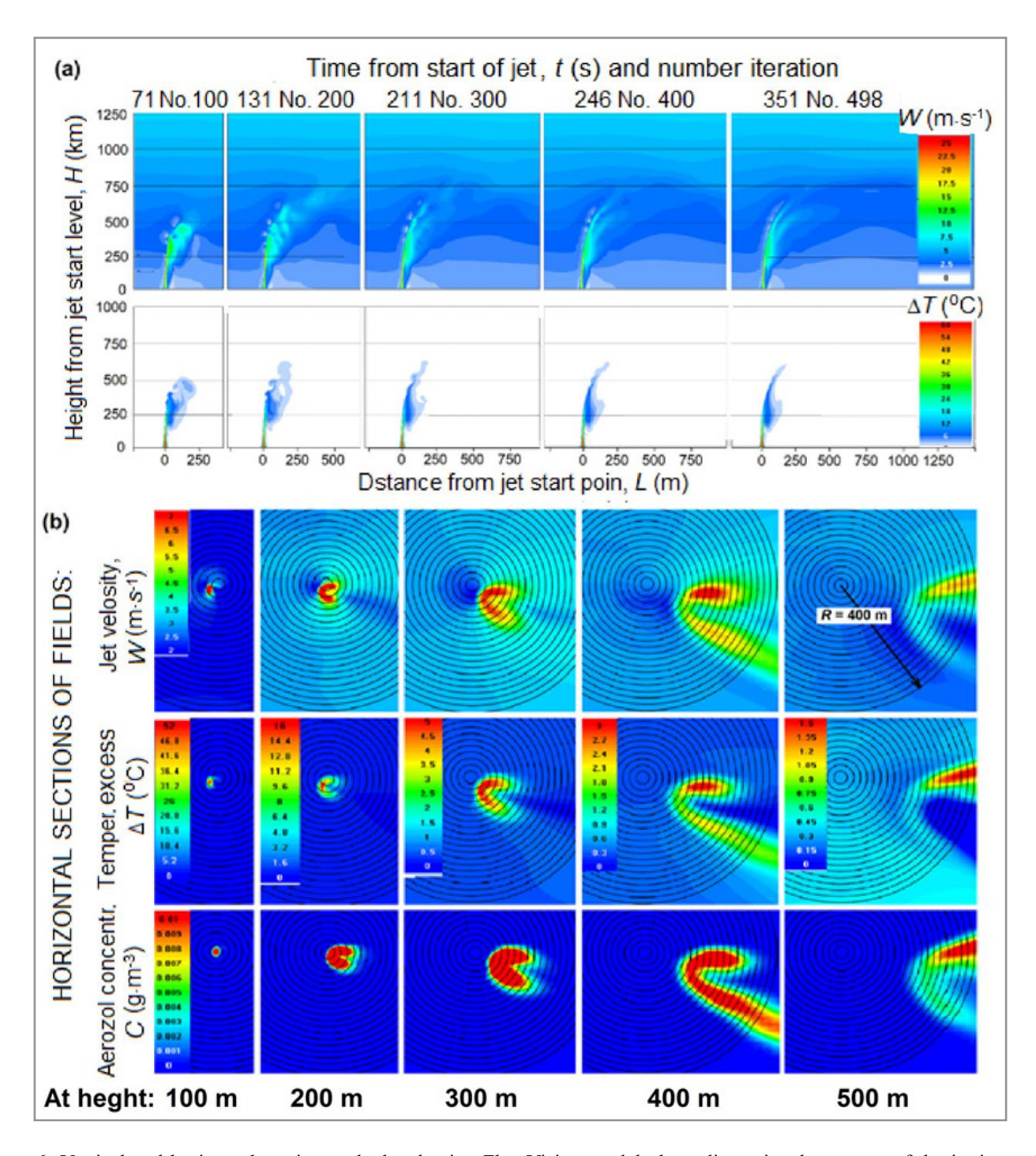


Figure 6: Vertical and horizontal sections calculated using FlowVision model, three-dimensional structure of the jet in a windy atmosphere: (a) - vertical cross-sections of jet velocity and temperature excess fields on 1, 2, 3, 4 and 5 minutes after start; (b) - horizontal cross-sections of the jet velocity, temperature excess, and aerosol concentration fields at altitudes of 100, 200, 300, 400 and 500 m. Atmospheric conditions: vertical wind speed profile U(H) = 1 + 0.004H, vertical temperature lapse rate $\gamma = 7.5$ °C.km⁻¹, air humidity RH = 45%.

- As the jet rises, it expands, loses superheat and loses its rate of ascent. The jet temperature drops faster than its velocity, so the top of the jet continues to rise by inertia until its temperature becomes equal or even lower than the ambient air temperature by 1.0-1.2 °C. Atomization of aqueous solutions of hygroscopic substances leads to a more rapid expansion of the jet, lowering its speed and temperature.
- Even a weak wind, increasing with height, leads to deformation of the jet, tilts and carries the top of the jet to leeward for hundreds of meters (Figure 6a). In the horizontal cross section, the jet takes the shape of an arc (figure 6b) encompassing a region of maximum upwelling that lags behind the surrounding airflow, similar to the lagging of the leading flow of the upwelling region and the powerful radar echo of convective storms [55]. Even a weak wind with a velocity of U = 1+0.005H reduces the jet lift height by almost half, which significantly limits the ability to create artificial clouds. This is one of the reasons for the modest
- results obtained in experiments with meteotrons by Dessens and Wolfson and Levin.
- The jet lift height increases as the vertical temperature gradient γ increases. Increasing γ from 6.5 to 9.5 oC/km increases the jet lift height by 60% (by 500-700 m) even with significant wind deformation of the jet.
- Increasing air humidity also increases the jet lift height due to the fact that moist air is lighter than dry air.

Fueling the jet with condensation heat markedly increases its lift height in the atmosphere. This can increase the potential to overcome inversion layers, reach the level of natural condensation and trigger the cloud formation mechanism. Figure 7 shows that increasing the PC boost energy by a factor of 2 and 4 increases the jet lift by 6% and 14%, respectively. In a windless atmosphere, the energized jet reaches high altitudes already at $\gamma = 6.5$ °C/km, and at $\gamma = 7.5$ °C/km it can reach the height of the condensation level (1200 m) and initiate cloud formation.

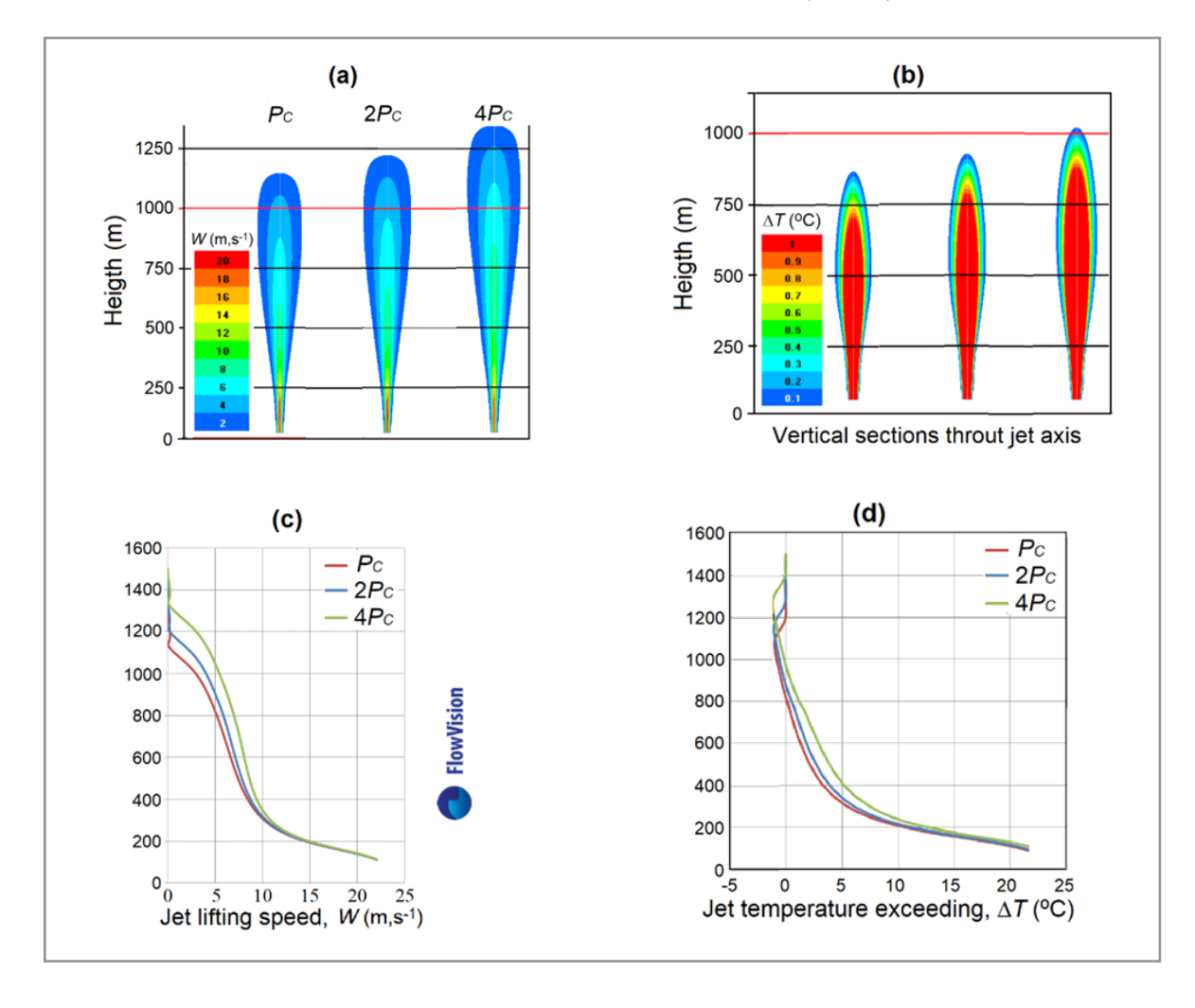


Figure 7: (a) and (b) - vertical cross-sections of the calculated fields of updraft velocity (W) and jet temperature excess (ΔT); (c) and (d) - vertical profiles of the maximum values of W and ΔT on the jet axis, which is fed by water vapor condensation heat equal to PC = 9.8 MW.c-1, 2PC and 4PC. Atmospheric conditions: wind speed U = 0; temperature lapse rate γ = 7.5 oC.km-1, RH = 75%.

Experimental Equipment

The experimental complex (figure 8) included:

- D-30 III series aircraft jet engine with air intake, upward jet turning device, fuel system, starting and control system;
- type I aqueous solution atomization system consisting of a solution tank and 80 nozzles mounted at the outlet of the jet turning device around the perimeter;
- two aerodynamic fogging guns JY-60 and WP-60 for spraying of aerosols of the second and third types with 20 kW

- fans, power supply and control systems, tanks for solutions of hygroscopic substances;
- system for preparation and storage of aqueous solutions of three hygroscopic substances;
- scientific equipment for monitoring the results of field experiments, which included (see figure 14): Vaisala WXT-536 weather station for measuring pressure, temperature, air humidity, wind direction and speed, intensity and amount of precipitation; Halo-Photonics Streamline XR Wind Lidar for measuring the vertical profile of wind direction and

speed; HATPRO RPG multichannel microwave radiometer for measuring the vertical profile of air temperature and humidity; IRTIS2000C thermograph for obtaining the thermal structure of the jet; hexacopter drone with onboard sensors kit for measuring jet in-situ temperature, humidity, pressure, aerosol concentration and 3-D wind. The readings of these instruments were complemented by data from the Abu Dhabi airport atmospheric radiosonde, the Meteosat-10 satellite and the local C-band weather radar.

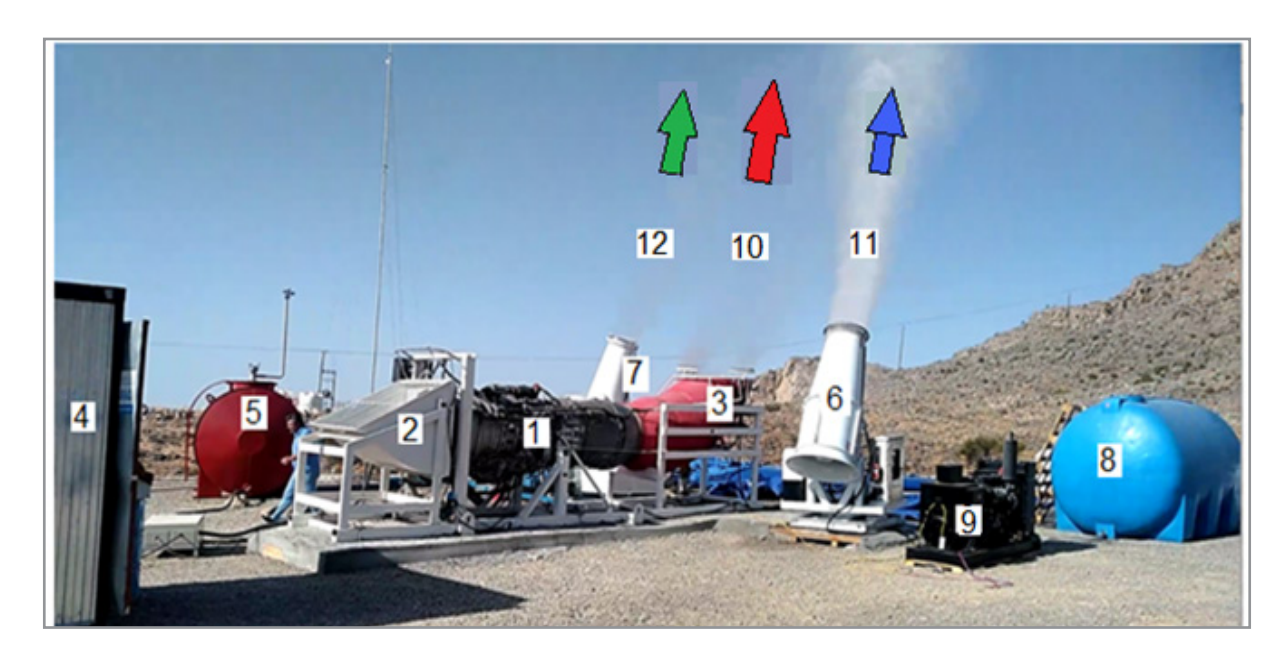


Figure 8: Experimental equipment on the Jebel Jais mountain in the UAE: 1 - turbojet engine D-30 III series; 2 - air intake; 3 - diverter serving to turn the jet upwards; 4 - cabinet with control system of D30 engine; 5 - tank for aviation kerosene; 6 and 7 - JY-60 and WP-60 aerodynamic cannons for spraying aqueous solutions of hygroscopic substances; 8 - tank for aqueous solution of NaCl; 9 - diesel generator 3x380 50 kW, powering the cannon JY-60; 10 - upward flow created by the engine D-30 (almost transparent); 11 and 12 - gas-droplet streams created by cannons JY-60 and WP-60.

The jet of the D-30 engine and the gas-drop streams of the JY-60 and WP-60 air guns were directed so that they merged into a single upward flow at a height of about 20-30 m. The initial parameters of this common jet were as follows: the initial jet temperature was about 300 °C and the flow rate was about 300 °C. The initial parameters of this common jet, taking into account losses in the turning device and on solution evaporation, were as follows: initial jet temperature about 300 °C, flow velocity about 300 m.s⁻¹, combustion products flow rate about 200 kg.s⁻¹, initial jet diameter 1.2 m, jet inclination angle to the horizon 75o.

Field Experiments and Their Results

In the first field campaign, the experimental complex was mounted on Mount Jebel Jais at an altitude of 1600 m from February 17 to March 12, 2021. Until the end of March (and according to the forecast and beyond), despite the readiness to conduct experiments, atmospheric conditions were unfavorable for the creation of artificial clouds. Low air humidity in the surface layer (11-25%), presence of surface layers of inversion, surface wind speed of 2-5 m.s⁻¹ were noted. Only in the layers above 3.5-4.0 km, the height of which the jet did not reach, sometimes humidity of about 50-60% was noted.

Despite unfavorable atmospheric conditions, 4 trial experiments on creation of artificial upward flows in a cloudless sky were carried out. The purpose of these experiments was to check the performance of the experimental complex and to study the peculiarities of the jet feeding by condensation heat. The experiments were conducted on March 15, 17, 23 and 24 from 14:30 to 15:45 local time (during the period of maximum natural convection). The duration of the experiments (in terms of jet engine operation time) was (9-15 min). On March 15, light layered puffy-puffy clouds were visible on the horizon, and on other days there was a clear cloudless sky.

Results of Trial Experiments

In none of the experiments was it possible to create an artificial convective cloud. In all experiments, only aerosol jets and translucent aerosol clouds were observed against a clear sky background (Figures 9c and 9d), which represent the air-drop flow produced by a JY-60 fog cannon spraying CaCl2 solution. Droplets of CaCl2 solution, vaporize in the hot jet, but after the jet cools down somewhat, droplets are again formed on the CaCl2 aerosol due to the low hygroscopic point (RH1 = 6%). In contrast, air-drop streams with droplets of (NH2)2CO and NaCl solutions became visually invisible after evaporation in the hot

jet, because for the reformation of droplets on aerosols of these substances in the atmosphere, the air humidity was below their hygroscopic points.

The jet temperature at the edge of the engine nozzle according to thermocouple measurements reached $275-300\,^{\circ}\mathrm{C}$ depending on the D-30 engine speed. It was not possible to measure the temperature and velocity in the center of the jet. The initial jet velocity at the jet edge at the beginning is about 300 m.s⁻¹. According to the jet flow theory [56], this means that the maximum jet velocity at the axis could reach $400-450\,\mathrm{m.s^{-1}}$.

The height of the rising jet according to the IRTIS-2000S thermograph data reached an average of 600 m and a maximum of

1100 m above the launch level (see figure 9). The upward flow velocity at a height of 400 m according to the meteorological drone data reached 3 m.s⁻¹.

The average background aerosol concentration during the day at 1.8 m height in the size ranges of 0.3; 0.5; 1.0; 2.5; 5.0 and 10 μm was 3255, 1156, 303, 67, 17 and 12 m-3, respectively.

According to the photoelectric pyranometer RK200-03, the solar energy flux on the flat surface was 0.85-1.0 kW.m⁻². The noise level of the machine's jet engine reached 132 dB SPL according to the MEGEAN 92131 noise meter, and 135 dB at maximum engine speed.

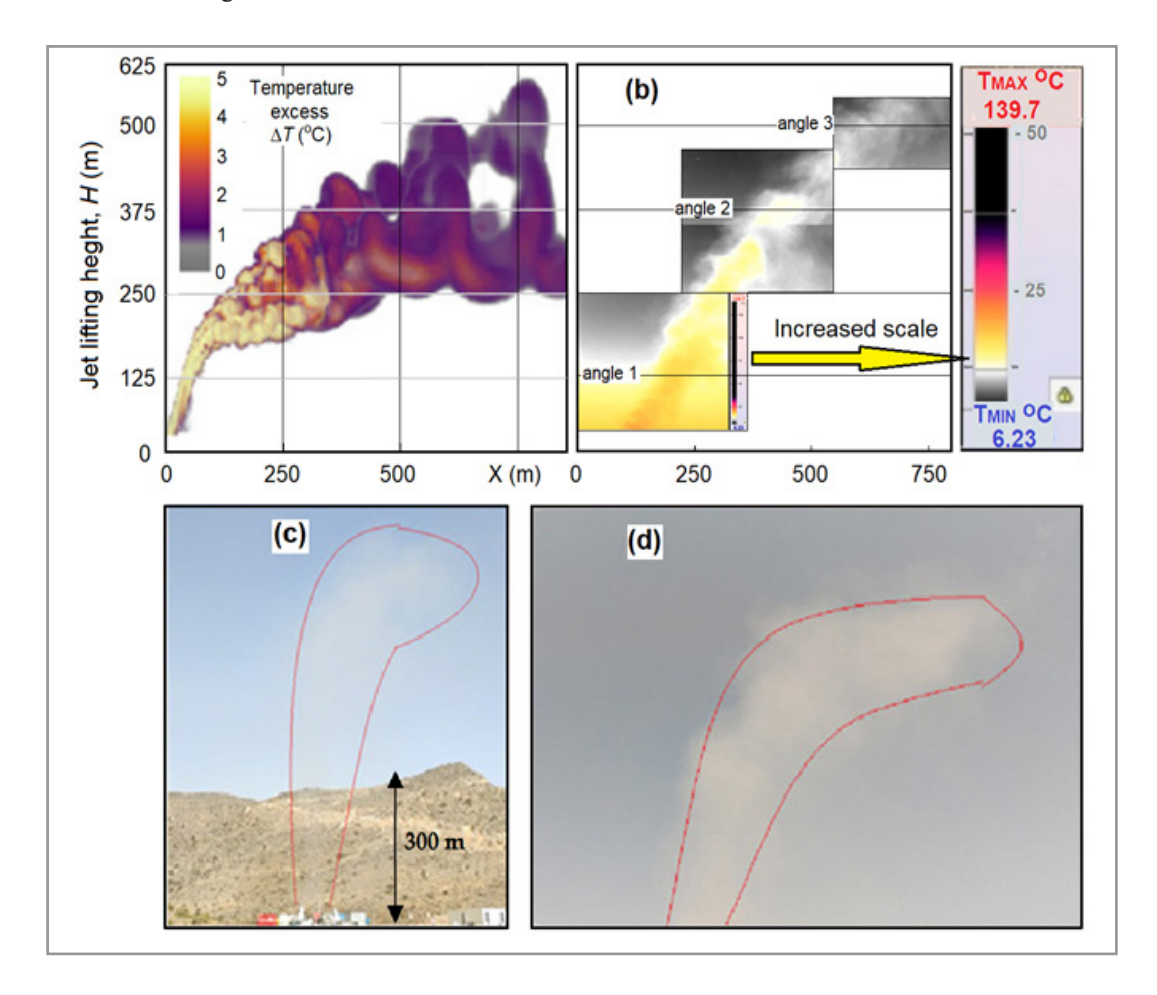


Figure 9: Comparison of the simulated and observed jet characteristics, initiated during a trial field experiment on Jebel Jais Mountain of UAE on March 17, 2021: (a) – jet shape calculated in FlowVision; (b) thermal images of the jet obtained with an IRTIS-2000C infrared scanning thermograph at 3 viewing angles; (c) – photo of the jet in the atmosphere; (d) photo of the upper half of the jet.

Results of Experiments in the Second Field Campaign

Atmospheric conditions during this field campaign were more favorable for the artificial cloud experiments. Between December 30, 2021 and January 5, 2022, large-scale cloud processes and precipitation were observed, especially intense over the sea surface in the west and east of the UAE Peninsula. The only factor complicating the selection of favorable conditions for the experiments was the increased wind speeds. Fifteen experiments were conducted in this campaign, including 13 experiments con-

ducted at Mount Jebel Jais (25, 26, 29, 30, and 31 December 2021, 3, 4, 5, and 7 January 2022) and two experiments conducted on January 15, 2022 in desert in the south of the UAE. Saturated solutions of three hygroscopic substances CaCl2, NaCl and (NH2)2CO were injected into the upward flow created by the jet stream, and on 5 occasions 20 kg of NaCl/TiO2 nano-powder and 50 kg of CaCl2 powder each were injected (see Table 3 in [57]. These 15 experiments were conducted under the following atmospheric conditions:

- 6 experiments under a cloudless sky;
- 2 experiments when cumulus clouds passed over the field site:
- 2 experiments when a layered cumulus cloud passed over the position;
- 2 experiments when layered cumulus clouds passed over the site:
- 3 experiments in the presence of second-tier layered cumulus and layered clouds (at altitudes above 3000 m) over the site and its surroundings;
- 2 experiments when layered cumulus clouds passed through the site and close to the ground level.

According to the results of instrumental control, the following effects were observed:

- in 6 cases formation of light almost transparent cloud in clear sky:
- in 3 cases compaction of layered clouds into which a jet saturated with hygroscopic aerosols was injected;
- in 3 cases appearance of the precipitation radar echo spot (figure 10c) on the leeward side 15-20 minutes after the launch of the jet-aerosol machine. This is probably connected with the impact of the jet directly on clouds of Cu Hum (2 cases) and St (1 case) types;
- in 2 cases convergence of small clouds of Cu Hum type in the direction of the jet.
- in 1 case no effects were detected.

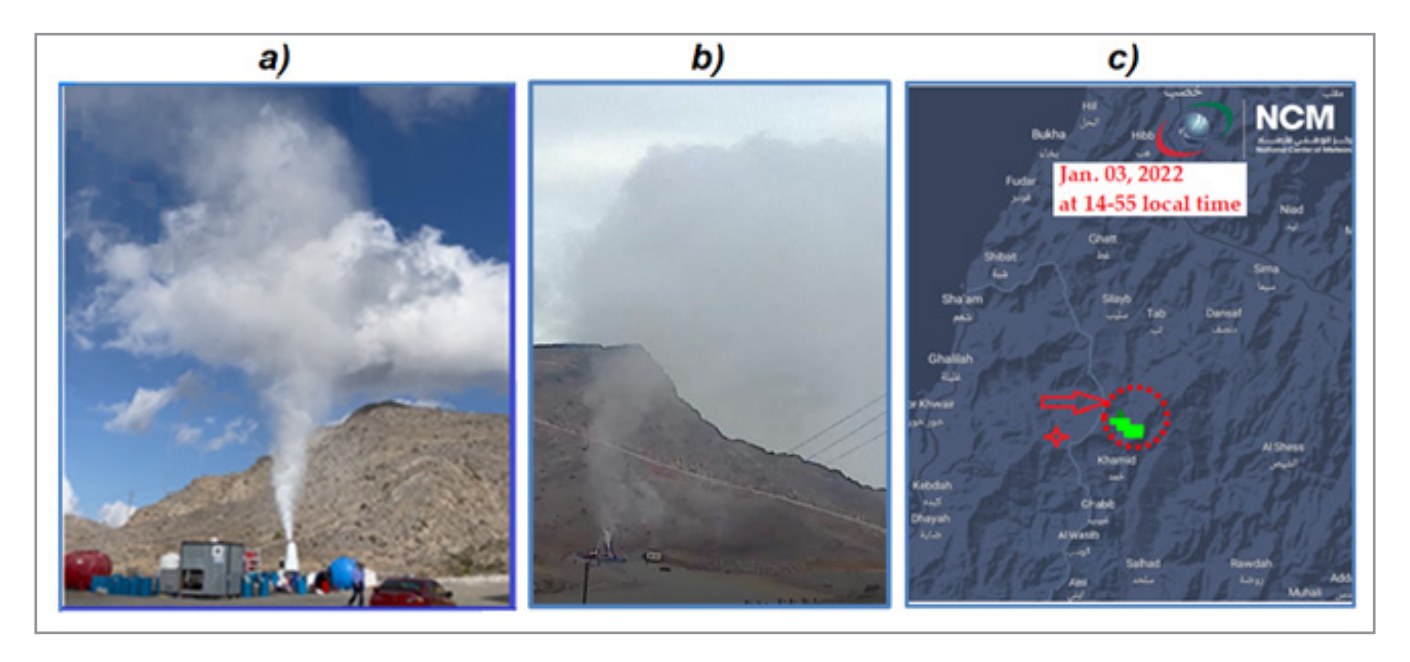


Figure 10: Artificial clouds and precipitation created by the vertically directed jet of the aircraft turbojet engine D-30 III series: a) cumulus cloud on the background of clear sky 28.12.2021; b) cumulus cloud on the background of layered cloudiness 31.12.2021; c) radar echo zone of artificial precipitation caused by 03.01.2022 (highlighted in green).

In no experiment was it possible to create deep convection with the development of an artificial convective cloud in clear skies. Enhancement of natural Cu Hum clouds and stimulation of local precipitation from layered cumulus clouds passing over the jet-aerosol intervention, are of no serious practical significance. These results are significantly lower than those expected on the basis of theoretical modeling for the case of a jet with energetic feeding, but they are in good agreement with the data of calculations for a jet without feeding [47, 51].

The analysis showed that the reasons for such modest results are that the expected enhancement of the jet energetics due to the heat feeding of water vapor condensation on the three types of hygroscopic aerosols introduced into the jet was too small due to the absence of condensation on (NH2)2CO), NaCl, NaCl/TiO2 aerosols because of the low humidity of the surface air (RH < 65%), and the amount of water condensed on CaCl2 aerosol according to Table 1 is small. First, the condensation process of water vapor on the hygroscopic aerosols introduced into the jet

is not so fast [58], to provide an energy makeup of the condensation heat during the jet ascent. Without such a feeding, the power of the used D-30 aircraft jet engine was not sufficient to initiate deep convection and create clouds producing heavy rainfall.

According to the data of modeling of jet motion in the atmosphere [47], it follows that even with a weak wind (U = 1+0.005H m.s⁻¹) and temperature lapse rate $~\gamma = 8.5~^{\circ}\text{C.km}^{-1}$ the D-30 engine jet cannot reach the level of cl loud formation without a feeding (see the left part of Figure 11). Increasing the engine power by 2, 4, 8 and 16 times leads to a significant increase in the volume of the jet and its height of ascent (up to 2500 m). This means that with sufficient engine power the jet can overcome inversion layers, destructive effect of wind, reach the level of condensation and lead to the formation of convective cloud, which under favorable atmospheric conditions (increased humidity and the presence of potential energy of atmospheric instability) can develop and lead to the formation of cumulus rain producing clouds.

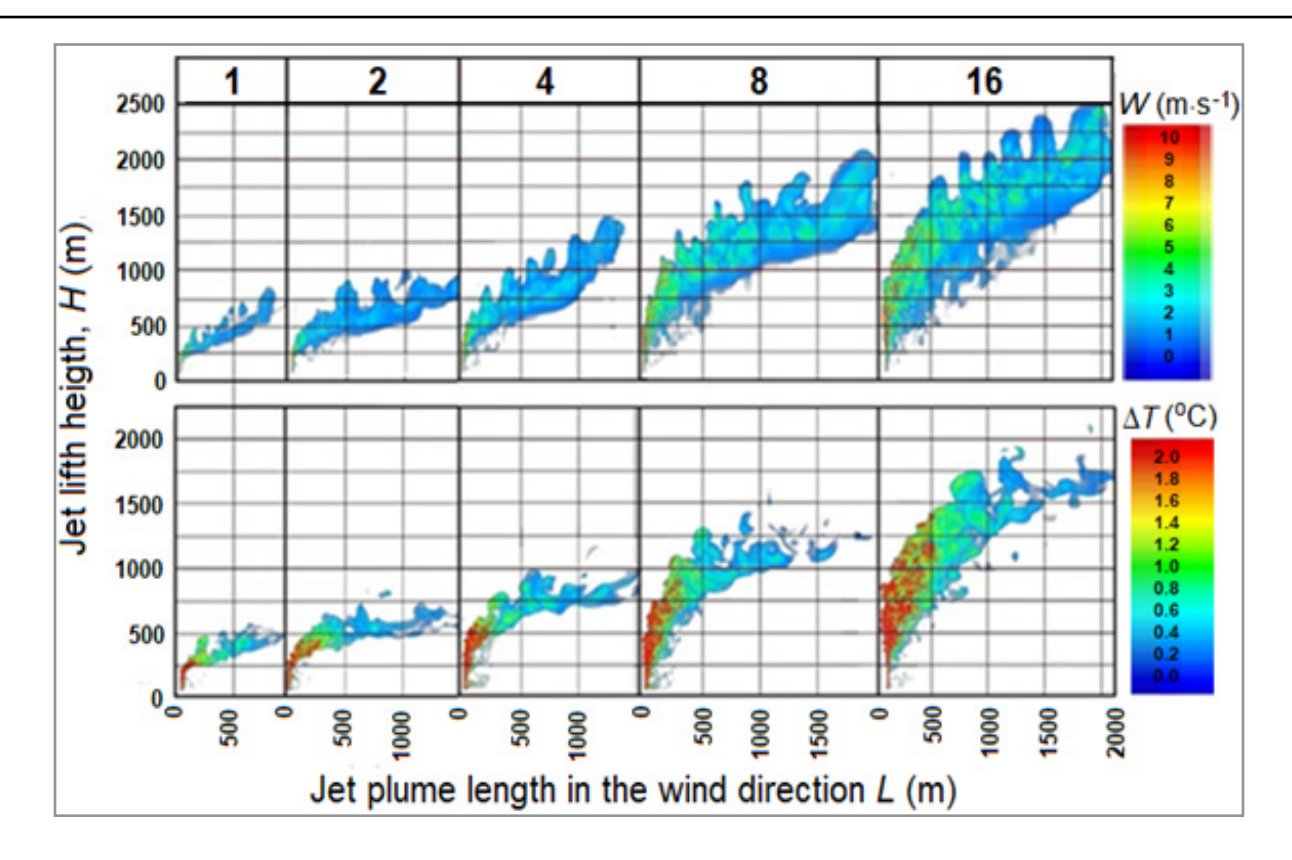


Figure 11: Vertical cross-sections of the calculated updraft velocity fields (W, m.s⁻¹) and excess of jet temperature (Δ T, oC) that can be created in the atmosphere by jet engines that have 1, 2, 4, 8, and 16 times the power of the D-30 engine. Atmospheric conditions: vertical wind speed profile U = 1+0,005H (m.s⁻¹), temperature $\gamma = 8.5$ °C.km-1; humidity RH = 70%.

Method for the Creation of Powerful Convective Clouds

The purpose of this method is to create a super powerful ascending jet of heated gases and water vapor that in suitable conditions can trigger formation of a deep convective cloud. The jet is directed to the zenith. Water vapor has an initial temperature of about 2700 – 3000 °C, initial flow velocity and rate make value about 4000 m.s⁻¹ and 1000 kg.s⁻¹ respectively. At least 1012 particles/s of hygroscopic aerosol with a diameter of about 5 microns are introduced into the jet in order to accelerate cloud and precipitation formation [48].

Atomization of hygroscopic aerosol is carried out at a height where the temperature inside jet becomes below the aerosol substance dissociation (melting) point. Saturation of the updraft with novel effective hygroscopic aerosol [51, 59], can promote acceleration of water vapor condensation and finally formation of rain size drops. To implement the method, a device containing an aerospace jet engine with an upwardly directed nozzle and an unmanned aerial vehicle is proposed to provide atomization of hygroscopic aerosol in the jet stream.

The Physical basis of the proposed method of inducing artificial rainstorms consists in the forced creation of a powerful upward flow saturated with hygroscopic aerosol, which rising in the atmosphere leads to the formation of an artificial convective cloud similar to those formed during bench tests of aerospace engines (see figure 12), despite measures to dampen the energy of their

jet. Such tests are carried out on complex large-scale test stands that include, for the safety of the exhaust gases for the surrounding urban environment:

- reducing the velocity of the reactive jet by changing the diameter of the pipes through which the jet flows, including the confuser, cylindrical pipe and diffuser;
- reducing the temperature of the jet stream by mixing it with nitrogen and atmospheric air blowing on the engine;
- reducing the temperature of the jet by injecting large amounts of water into the jet at the inlet of the confuser and at the inlet of the diffuser;
- jet velocity reduction due to jet rotation in the gas dynamic tube and gas dynamic unit;
- reduction of jet kinetic energy by abrupt expansion in a hydrodynamic carrier;
- reduction of kinetic energy of the jet in a vertical diffuser tube with a height of about 80 m and a diameter of 15 m.

After all these manipulations, the jet, which had supersonic velocity and very high temperature, is ejected into the atmosphere with a multiply reduced velocity and temperature. But even this is sufficient for the formation of powerful convective clouds with a height of several kilometers (Figure 12). In 15-25 minutes after engine operation termination, these clouds usually dissipate, giving small precipitation, and under favorable atmospheric conditions can grow into powerful cumulus-rain clouds.

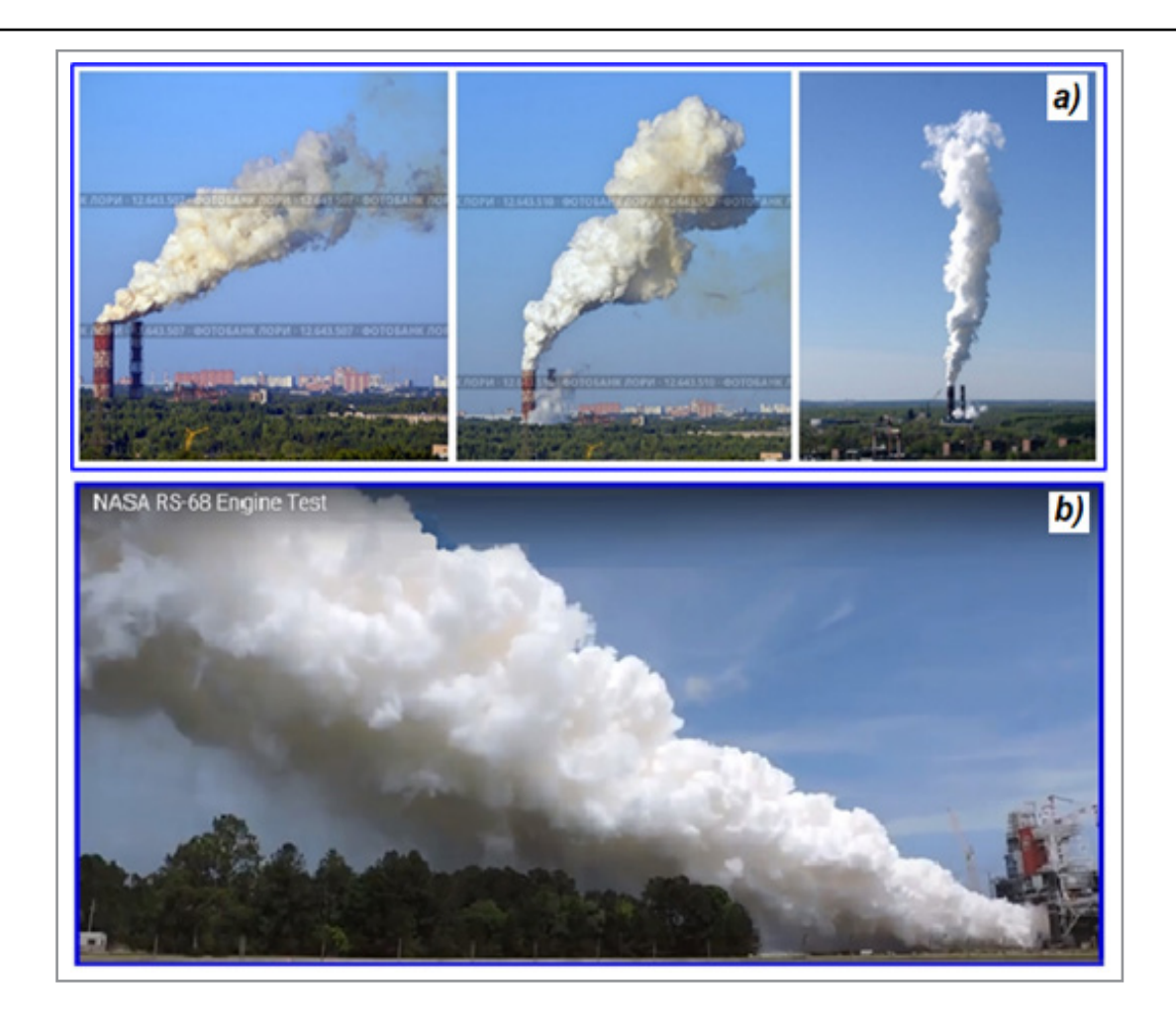


Figure 12: Artificial clouds formed by breakthrough gases during testing of aerospace rocket engines: (a) - Moscow Region, Khimki, NPO Energia (Internet resource). (b) - Artificial cloud with a little rain formed during the test of the engine of the super-heavy RS-68 carrier rocket [60], at NASA's Mississippi Space Center. (https://youtu.be/aXLZAfYgbM4 [31].

Device for Inducing Artificial Rain

To induce formation of a deep convective cloud it is proposed to use special device containing an aerospace jet engine, tanks with liquid fuel and liquid oxygen, an unmanned aerial vehicle with a sprayer of hygroscopic powder and a set of instruments for measuring the parameters of the atmosphere, jet stream and artificial cloud medium. The most acceptable for these purposes is a liquid oxygen-hydrogen engine of RD-0120 type and its analogs, whose exhaust mainly contains cloud forming water vapor. Also acceptable are three-component oxygen-kerosene-hydrogen engines such as RD-0750, RD-704, or oxygen-methane engines such as RD-0169 and their analogs. More powerful engines like RD-170, RD-171 can be very efficient for creating artificial clouds, but they have high fuel and oxidizer consumption.

Test experiments can also be carried out using oxygen-kerosene engine NK-33 and its analogues (NK33/AJ26, NK43, AJ26-58, AJ26-62, etc.) having thrust of 154 tons, an operating time of up to 365 seconds, a length of 3705 mm, a diameter of 1490.5 mm, a dry mass of 1240 kg, the possibility of multiple use and high reliability of operation of 0.9994 [62].

In contrast to its direct purpose, the NK-33 engine is mounted on a solid fixed support with the nozzle upwards, so that a jet of gases with an initial temperature of about 2000 °C, a velocity of 3000 m.s⁻¹ and a mass flux of more than 2200 kg.s⁻¹ creates an extensive upward flow and initiates the formation of a powerful convective cloud. The operation time should be about 150-300 seconds to create an initial convective cloud with a volume of at least 106 m3. Under favorable conditions (high air humidity, weak wind), such a cloud can develop due to the release of water vapor condensation heat and the potential energy of convective atmospheric instability (CAPE). The introduction of a hygroscopic aerosol, such as novel core/shell NaCl/TiO2 [59], with a diameter of about 5 µm at a dosage of about 1012 particles.s⁻¹ (about 0.1 – 0.2 kgs⁻¹) into the jet can lead to a lowering of the condensation level and acceleration of the water vapor condensation process and, ultimately, to the formation of rain [62].

Aerosol application is carried out by spraying hygroscopic powders from an unmanned aerial vehicle such as those used for spraying fields, hovering in the center of the jet at an altitude of 400-500 m, where the temperature of the jet according to the on-board sensor will become lower than the dissociation threshold of the aerosol substance. Aerosol can also be introduced by spraying an aqueous solution of hygroscopic substance into drops of 10-15 microns in diameter, which instantly vaporize to form an aerosol of 5-10 microns in diameter.

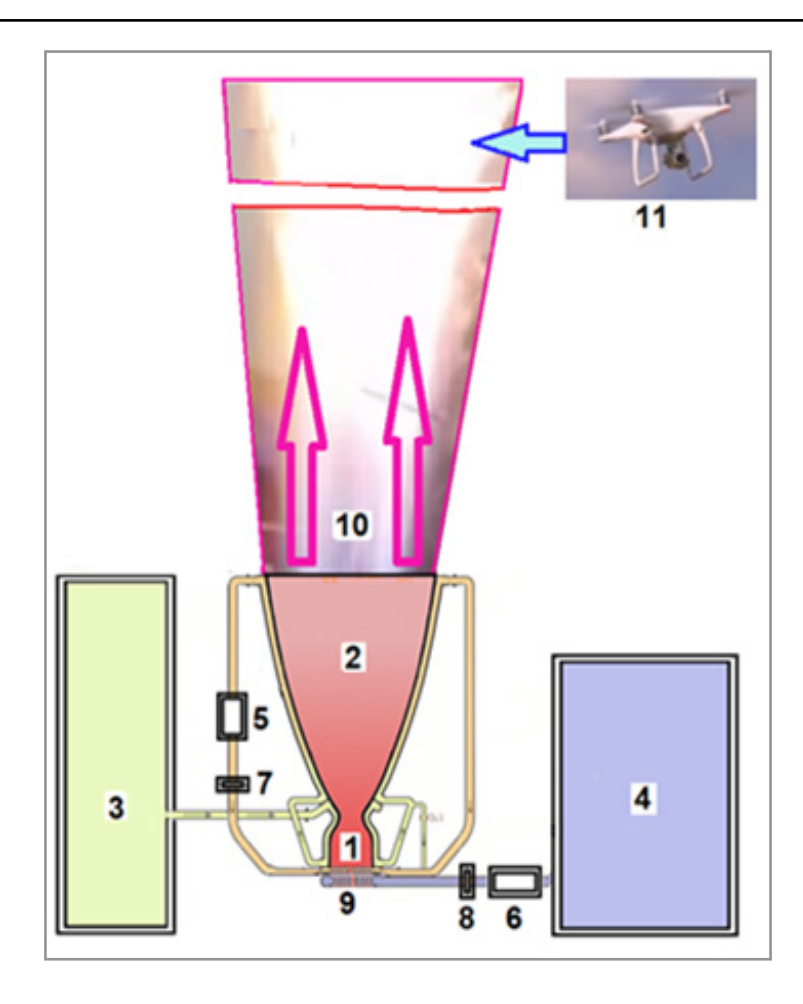


Figure 13: Simplified scheme of the experimental Device for inducing cloud formation: 1 - combustion chamber; 2 - jet gas flow nozzle; 3 and 4 - tanks for kerosene and liquid oxygen; 5 and 6 - high-pressure turbopump units for fuel and oxygen supply; 7 and 8 - pneumatic valves for fuel and oxygen shut-off; 9 - ignition device; 10 - high-temperature high-speed water vapor jet; 11 - drone for introducing hygroscopic aerosol into the water vapor jet.

Figure 13 shows a simplified scheme of a device for inducing cloud formation, which contains a combustion chamber (1), a nozzle directed to the zenith (2), tanks for kerosene and liquid oxygen (3) and (4), high-pressure booster turbopumps (5 and 6)

that supply kerosene and liquid oxygen to the combustion chamber through valves (7 and 8), an ignition device (9), and a drone (11) that introduces hygroscopic aerosol into the jet (10) at a safe altitude (400-500 m).

Table 2: Evaluation parameters of the jet created by NK-33 engine

No.	Parameter	Designation	Unit of measurement	Value
1	Initial jet temperature	T_{o}	°C	1700
2	Initial velocity of jet gases	W_{o}	m.s ⁻¹	3000
3	Initial mass flow of jet gases	$m_{_{o}}$	kg.s ⁻¹	2200
4	Initial jet diameter at nozzle outlet	$d_{_{o}}$	M	1,49
5	Pressure in the jet at the nozzle outlet	$p_{_{o}}$	kg.cm-2	0,4
6	Jet power	P_{o}	MW	5000
7	Volume flow rate of gases at nozzle outlet	$v_{_{o}}$	m3.s ⁻¹	5500

The experimental Device also includes a set of meteorological instruments (figure 14) for measuring the parameters of the atmosphere, jet stream and artificial rain, based on the data of

which the decision is made to conduct rain inducing operations and assess their effectiveness.

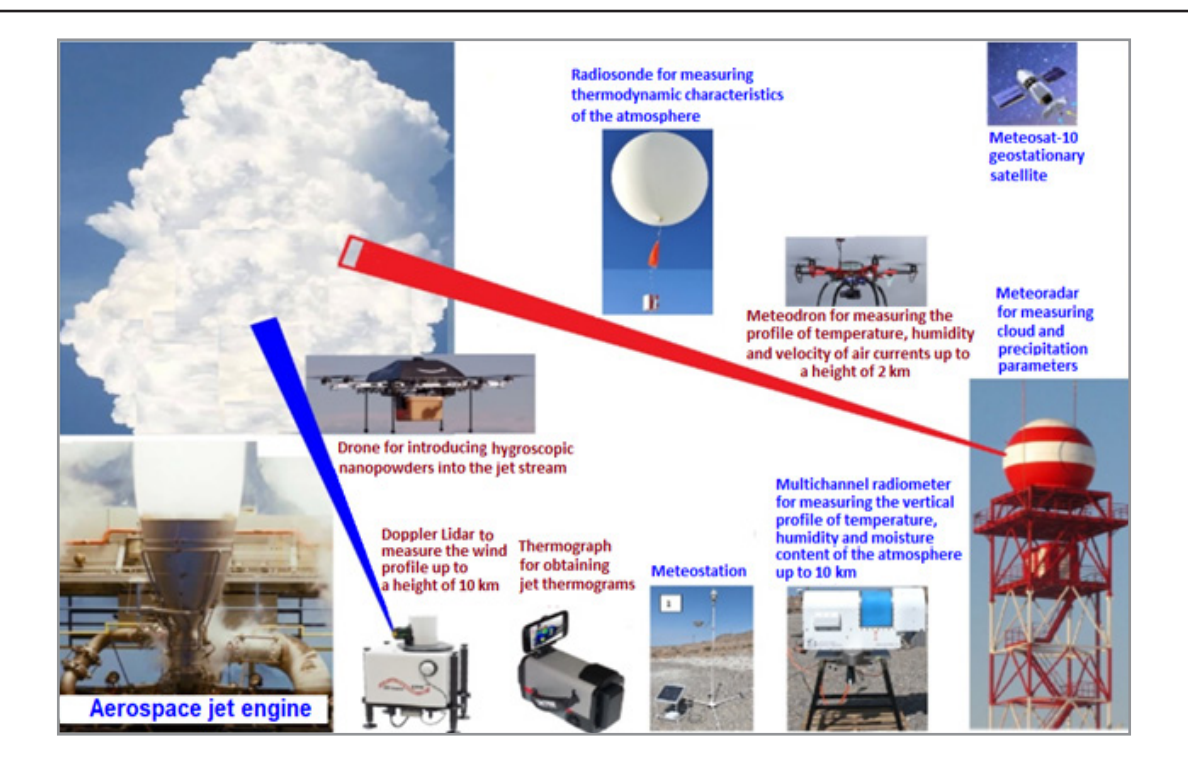


Figure 14: Complex instrumentation for measuring atmospheric parameters, characteristics of artificial upwelling flows, clouds, and precipitation.

The proposed Device is created on the basis of existing industrial samples of aerospace engines, unmanned aviation and measuring equipment. For large-scale application and cheapening of the Device it is envisaged to develop a simplified version of the jet engine, which provides for exclusion of design elements serving for application on carrier rockets

Study of Aerospace Engine Jet Parameters

The proposed Device is created on the basis of available industrial samples of aerospace engines, unmanned aviation and measuring equipment. However, for large-scale application and cheapening it is envisaged to develop a simplified version of the engine, in which it is envisaged to exclude the design elements necessary for its application on carrier rockets. In addition, it was planned to modify the nozzle design in such a way as to provide vortex rotation and wide-angle jet flow. The large initial velocity of the aerospace engine jet (W0 = 3000 m.s⁻¹) leads to large losses of its energy to overcome the resistance of the medium, proportional to the square of the velocity.

For CFD modeling of the jet motion in the atmosphere, the FlowVision software package was used. Calculations of the jet parameters in the initial period were performed in a fully compressible formulation, since the density and velocity of the jet at the exit of the engine nozzle and in the Mach, barrels reach 4-5 M. After the jet velocity decreased to 0.5 Mach, the calculations were performed in a special formulation of local atmospheric currents [47].

A study of the possibility of reducing drag losses by widening the jet in the diffuser from the standard angle $\theta_0 \simeq 2$ degrees to $\theta=25$ degrees has shown that this gives a slight reduction in jet velocity losses up to a height of 300 m, and above 400-500 m the jet loses its original width and according [63], acquires a width of about 22.5 degrees. Changing the initial width of the jet does not change the height of the jet rise. It is also found that the highspeed jet has a counter clock wise vortex rotation. Therefore, there is no need to change the standard nozzle design.

CFD modeling showed that the jet of the RD-0120 aerospace engine with a standard nozzle can reach a height of 4-7 km depending on the value of vertical gradients of temperature, humidity and wind speed (Figure 15).

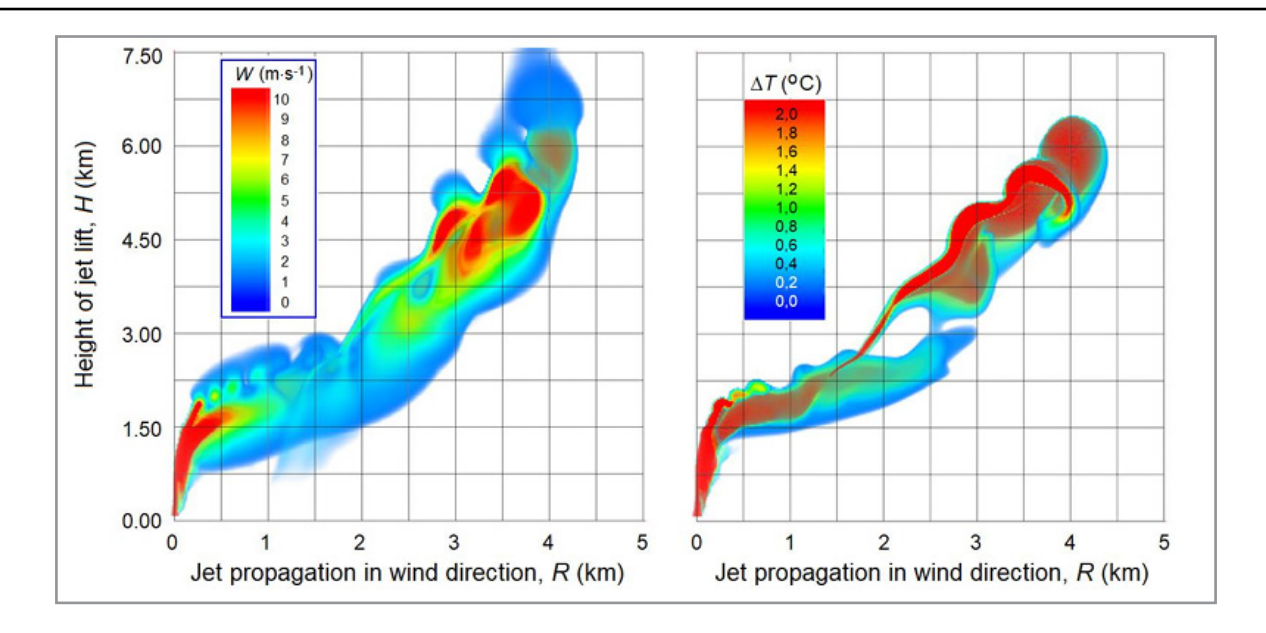


Figure 15: Vertical cross section of the velocity and temperature fields of an aerospace engine jet calculated using the FlowVision CFD model at operating time of 350 s, water vapor flow rate M = 1100 kg s-1, vertical temperature profile $\gamma = 7.5 \text{ °C km-1}$, wind speed U(H) = 1+0.005H m s-1, and air humidity RH=75%.

Selection of Position and Favorable Atmospheric Condition

It is obvious that triggering cloud formation of significant intensity and scale can be realized only in places and days with favorable atmospheric conditions. Natural convective clouds with showers are formed in meso-areas of favorable combinations of pressure, air temperature and humidity, terrain, wind speed and direction. Such favorable combinations are rare in arid and desert regions. It is assumed that proposed method may in some cases expand the range of meteorological conditions when rain producing clouds form in nature by affecting the atmosphere with a short-term but energetically powerful pulse capable of triggering the action of its own potential energy of atmospheric instability.

Selection of a Favorable Position: It is expedient to locate the Device for cumulonimbus clouds creation on the seashore on the windward flank of the coastal elevation to, firstly, initiate the upward flow from the surface layer of the atmosphere having maximum water vapor content, and, secondly, the breeze and orographic circulation can promote the development of artificial convection initiated by the powerful jet stream. High humidity of sea air, breeze and orographic convection will create a synergistic effect of increasing the buoyancy of the jet and the probability of cumulonimbus cloud formation. It is also reasonable to locate the device in mountains, in the headwaters of catchment basins of large rivers flowing to arid areas and feeding drying lakes such as the Aral in Central Asia, Urmia and Hamun in Iran and others. This will allow utilization of existing water collection and distribution systems.

The Device should be located no closer than 1000 m from populated areas so that the noise impact of the engine does not exceed the permissible sanitary level. Fuel tanks and tanks with liquid oxygen, a complex of equipment for measuring atmospheric parameters, artificial upward flows, clouds and precipitation, a site

for takeoff and landing of a meteo drone and a drone for aerosol spraying are located at a safe distance from the engine stand.

Selection of Days with Favorable Atmospheric Conditions: Theoretical and experimental studies of the motion in the atmosphere of a vertically directed jet stream [51], as well as the influence of parameters of the surface layer of the atmosphere on the development of cloud convection [37, 45, 64], have shown that favorable conditions for the creation of artificial rainfall are:

- surface wind speed not more than 2 m.s⁻¹, in the layer up to 1000 m not more than 6-8 m.s⁻¹;
- surface air humidity RH > 70%;
- thickness of surface air temperature and humidity inversion layers Δh < 500 m;
- potential energy of instability CAPE > 200 J/kg.
- The criteria for selecting days with favorable conditions are presented in Figure 15.

Favorable Synoptic Situations are considered to be the presence of the area of low pressure and convergence with the cold inflow at the heights, and also the intrusion of cold fronts contributing to the orderly ascent of warm air along the cold boundary.

The favorable Time of Day is the period of maximum atmospheric heating from 15-00 to 17-00 local time. This is due to the fact that the maximum solar radiation is observed at 12 o'clock, the maximum soil temperature comes in 1.5 - 2 hours, and the maximum surface air temperature is about 15 hours.

The Duration of the Device Operation can be from 150 to 300 seconds depending on the time of appearance of a powerful developing convective cloud. The intensity of cloud and precipitation formation increases with increasing duration of jet engine operation. However, the high fuel and oxidizer costs require a reasonable approach to determining the optimal duration of its operation.

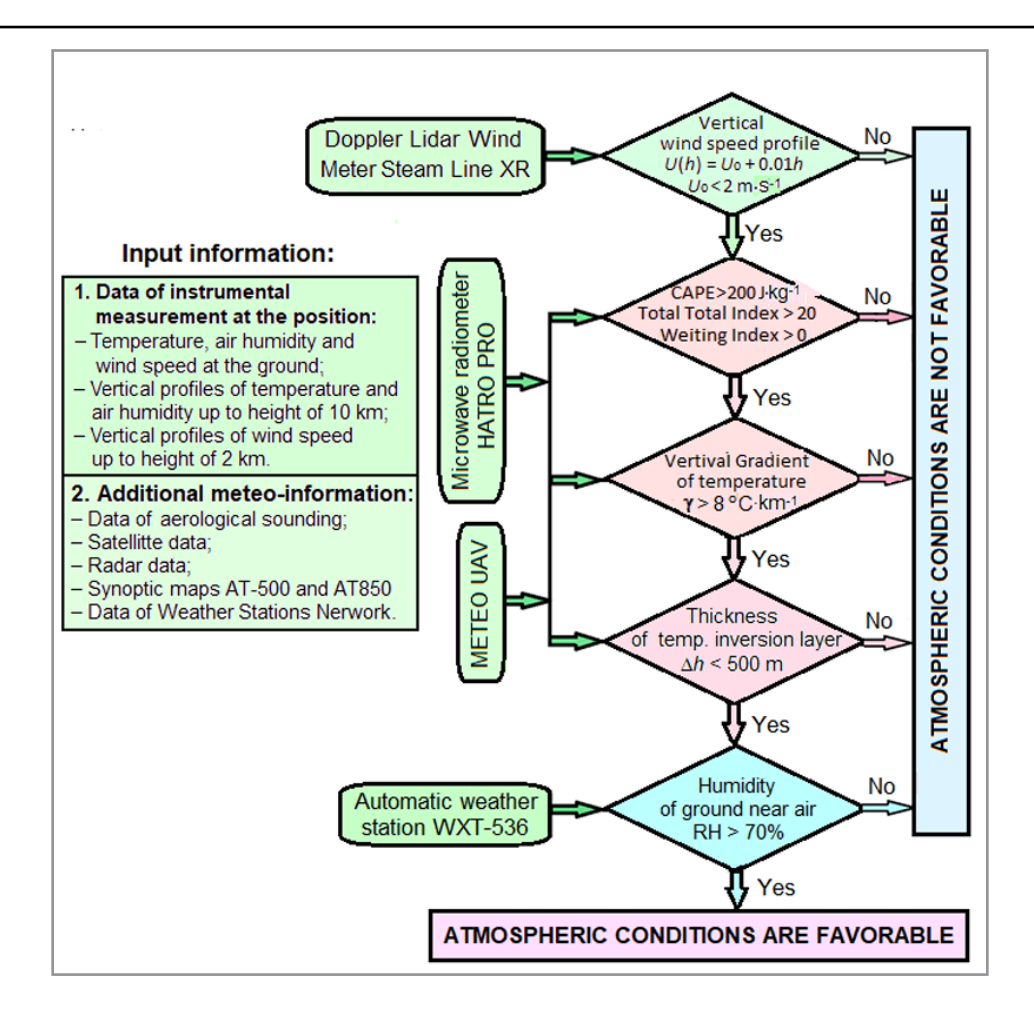


Figure 15: Flowchart for selecting days with favorable atmospheric conditions for creation artificial clouds and precipitation.

Assessment of the Expected Effectiveness of the Method

Natural clouds and precipitation are formed under favorable conditions characterized by some favorable combinations of the spatial structure of pressure fields, temperature, air humidity, wind direction and speed, the action of dynamic factors and orography. The spatial and temporal heterogeneity of the listed characteristics of the atmosphere creates a wide range of situations among which favorable conditions for the formation and development of clouds of certain types can be formed in some points of space in some periods of time. Our experiments on creation of artificial convective clouds by local impact on the atmosphere can be carried out in the conditions formed in the chosen place and at the chosen time. This sharply limits the choice of favorable situations, despite taking measures to optimally select the place, time, and atmospheric conditions.

An objective assessment of the effectiveness of the proposed method can be made on the basis of a series of full-size well controlled field experiments. But it is reasonable to assume that the proposed precipitation enhancement method may be more effective than the applied aircraft, rocket and ground-based methods of seeding existing clouds, which are scarce in desert regions. The proposed method can be used both to enhance existing clouds and to create artificial clouds on days when the formation of natural clouds is constrained by the presence of inversion layers, insufficient CAPE instability energy, and others. The selection of favorable atmospheric conditions, favorable position and time of day, and an engine of sufficient power increases the probability of creating artificial clouds and precipitation.

The proposed method also has advantages over commonly used technologies for seawater desalination, underground groundwater extraction, and underground seawater extraction, including:

- hundreds of times lower capital costs for infrastructure construction;
- ease and speed of infrastructure construction even in desert regions;
- reduction of water production costs by 2-3 times.

According to Internet data, the cost of building desalination plants with a daily capacity of 5×105 to 1×106 m3 in Saudi Arabia, UAE and Australia was \$1.5-2.0 billion. Construction of even 20 pcs. of the proposed Rainmakers, for example, along the entire northwest coast of the UAE would require about \$80 million. The infrastructure for such a system can be built in 1.5-2 years, while the construction of a 4.1×105 m3 per day Victorian Desalination Plant for Melbourne's water supply cost \$2.7 billion and took 3 years to build after a lengthy design.

The annual cost of operating the 20 proposed Devices, assuming about 25-30 stormwater generation operations at each, would be about \$90 million, of which about 60% would be spent on liquid oxygen and fuel (kerosene, hydrogen, or propane). As a result of 500-600 operations per year, about 5×108 m3 of fresh water can be obtained, considering that one heavy rainfall gives on average about 106 m3 of rainwater [55, 65]. At the same time, the cost of water, taking into account capital costs for construction and operation will be about 0.34 \$m-3, and taking into account only operational costs 0.18 \$.m-3.

The cost of seawater desalination, treatment and reuse of municipal wastewater, irrigation, and ballast water according to [10, 11], is about 4-7 times more expensive than the proposed technology and 3-5 times more expensive than traditional water

supply from rivers and lakes (see Table 4). The cost per cubic meter of water of the most advanced desalination plant Rabig-3 in Saudi Arabia is 0.53 \$.m-3.

Table 3: Cost of water produced by different methods (excluding capital costs)

Alternative water supply	Cost of w	vater \$.m ⁻³	Energy consumption (kWh.m ⁻³)
	limits	average	
Conventional surface water treatment	0.2 - 0.4	0.3	0.2 - 0.4
Water reclamation	0.3 - 0.6	0.45	0.5 - 1.0
Non-potable reuse	0.5 - 0.8	0.65	1.5 - 2.0
Direct potable reuse	0.7 - 1.2	0.95	1.7 - 2.4
Brackish water desalination	0.4 - 1.5	0.95	1.0 - 1.5
Seawater desalination (reverse osmosis)	0.5 - 2.5	1.5	2.5 – 4.0
Water collection from fogs	1.4 – 16.6	2.5	-
Application of the proposed Device	0.15 - 0.20	0.18	0.005

It should be noted that the advantage of desalination plants is the possibility of daily production of fresh water, while artificial heavy rainfall can be induced only on days with favorable atmospheric conditions. But the important advantages of the proposed method are lower cost of water, hundreds of times lower capital construction costs, and the possibility of quickly establishing a network of facilities that can cover large areas of deserts. Due to this, the proposed method can be an additional source of water, which is advantageous to apply in desert regions, including for groundwater recharge.

Potential consumers can be countries of Africa, Asia, North and South America, Australia. Taking into account these prospects, it is planned to produce an experimental sample of the proposed Device, to conduct demonstration experiments, to develop a simplified industrial sample of the Device and to conduct further research on the development of the scientific base and assessment of the consequences of the method application [66-73].

Conclusion

In result of theoretical and experimental studies of the possibility of creating artificial clouds and rain based on three different physical approaches, the following has been established.

1. A solar meteotron, which is an artificial aerosol layer created in the surface layer of the atmosphere using special pyrotechnic smoke bombs generating aerosol with a diameter of about 200 nm (see figure 1), well absorbing solar radiation in the visible wavelength range, can initiate thermal convection and the development of convective clouds of Pyro Clouds type at low surface wind speeds, vertical temperature gradient of more than 8 oC.km⁻¹ and increased air humidity. Experiments with the developed smoke bombs have shown that this is possible when the aerosol layer area is about 5-10 km2 and the concentration of aerosol particles is not less than 2.5×1013 m-2. Such concentration should be maintained for about 30 minutes or more. One operation to create an artificial cloud requires the consumption of aerosol composition in the amount from several tons to 20

- tons, depending on the dispersibility of the aerosol and wind characteristics. Therefore, the application of this method is very expensive and is only acceptable away from residential areas due to atmospheric pollution.
- The method of creating a jet of upward flow by means of a 30-40-tiered garland of black toroidal-shaped screens lifted on a balloon has no prospects for the following reasons. Even if the area of each screen is about 200 m2, the amount of absorbed solar radiation is so small that the upward flow pulse initiated by each tier does not reach the next tier due to wind drift and adiabatic cooling. This precludes the creation of a single upward flux by adding the pulses generated by all tiers. In addition, trial experiments have shown that the large sailing of the screens excludes the lifting of the garland consisting of more than 4-5 tiers even at wind speeds of 1-2 m.s⁻¹.
- 3. Field experiments on the creation of artificial clouds using a vertically directed jet fueled by the heat of water vapor condensation on three types of hygroscopic aerosols having different hygroscopic points showed the possibility of creating under some atmospheric condition's small artificial clouds and precipitation of no practical significance. The reason for these modest results is that the air humidity on the days with the experiments was lower than the hygroscopic point of the two types of aerosols (NaCl and (NH2)2CO) introduced into the jet at the start. Secondly, the condensation of water vapor on these types of aerosols was not so fast. Therefore, the jet did not receive the energy boost from condensation heat that we expected, and the power of the aircraft engine used was not sufficient to overcome the inversion layers and the destructive effect of the wind and create more powerful clouds.
- 4. Numerical modeling of jet motion in the real atmosphere based on the FlowVision 3-D hydrodynamic model has shown that even a weak wind increasing with altitude carries away the jet of an aircraft engine and it does not always reach the height of the condensation level.

Therefore, to create Cb-clouds, it is proposed to use a multiply more powerful aerospace engine mounted on a fixed support with the nozzle upwards so that the high-temperature jet creates a powerful upward flow. According to CFD modeling, such an upward flow reaches a height of 4-7 km and initiates the formation of a powerful artificial convective cloud, which is often formed during bench tests of aerospace engines.

Under favorable conditions (high air humidity, weak wind), such a cloud can develop due to the latent energy of atmospheric instability. Introduction of hygroscopic aerosol, for example, NaCl/TiO2 nano-aerosol with a diameter of about 5 microns at a concentration of at least 1012 particles/second into the jet stream can lead to acceleration of the process of heavy rain formation. Details of realization of this method, composition of the device and conditions of its application are described in Section 5.5.

In the future, it is planned to search for an investor and conduct field experiments to test the effectiveness of the method using aerospace engines, unmanned aircraft and nano-powders.

An important element is also the assessment of the environmental safety of the release of reactive gases into the atmosphere. In the case of RD-0120 type hydrogen-oxygen engines, the jet stream mainly consists of water vapor, which forms clouds. When using NK-33 type kerosene-oxygen engines, burning about 150 tons of kerosene and 400 tons of liquid oxygen in one operation to create artificial rain clouds (in 300 seconds) generates about 156 tons of water vapor, 468 tons of CO2 and about 6 tons of other gases (NOx, CO, SO2). With the large-scale application of the method with about 500 such operations per year, CO2 emissions will reach 2.35×105 tons, and the volume of CO2 emissions in the United Arab Emirates in 2021 amounted to 2.6×108 tons (i.e. 1,100 times more). Global emissions have reached 33.9 billion tons. (Source: CO2 total emissions European Commission, ED-GAR. Accessed on 1 September 2022). Therefore, the emissions of the proposed rainmaking method are negligible compared to other emissions. In addition, these emissions will mostly be washed out by artificial rains.

Data Availability Statement

The main results of the study are included in the article. Additional materials are available upon request.

Author Contributions

Both authors jointly carried out theoretical and experimental studies on the implementation of the described methods. MT developed the physical principles and concepts, interpreted the results of the field experiments, and prepared the manuscript. AM provided project management, collection and processing of instrumental data, validation of results and preparation of the final manuscript.

Funding

This work was supported by the National Center of Meteorology, Abu Dhabi, UAE under the UAE Research Program for Rain Enhancement Science (grant No APP-REP-2017-02120).

Acknowledgments

The authors express their gratitude to the group of specialists of TESIS Engineering Company represented by Dr. Aksenov A.A., Fisher J.V. and Shchelyaev A.E. for participation in the project

in terms of theoretical modeling at all stages of the project, as well as to the group of scientists of the North Caucasus State University represented by Professor Zakinyan R.G. and Associate Professor Zakinyan A.R. in terms of modeling the possibility of initiating artificial convection and favorable atmospheric conditions.

Conflict of Interest

The authors declare no conflict of interest.

References

- 1. Chowdhury's Guide to Planet Earth (2005). "The Water Cycle". West Ed. Archived from the original on 2011-12-26. Retrieved 2006-10-24.
- 2. Masson-Delmotte, M., Zhai, P., Partner, H.O. (2018). Global warming of 1.5 °C. Intergovernmental Panel on Climate Change.
- 3. Trenberth, K.E., & Jones, P.D. (2007). Chap 3, Observations: Atmospheric Surface and Climate Change, Executive Summary, p. 237 in IPCC AR4 WG1.
- Cook, K.H., & Vizy, E.K. (2015). Detection and Analysis of an Amplified Warming of the Sahara Desert. Journal of Climate, 28, 6560. https://doi.org/10.1175/JCLI-D-14-00230.1
- 5. UNESCO and World Water Assessment Programme (WWAP). (2017). The United Nations World Water Development Report 2017: Wastewater, The Untapped Resource. Paris: UNESCO.
- Petrov, V.I., Pavlovsky, V.S., Kulik, K.N., Voronina, V.P., & Skurko, V.E. (1999). Atlas of desertification of agricultural lands of the Russian Caspian Sea. Volgograd: VNIALMI.
- 7. Dedova, E.B., Goldvarg B.A., & Tsagan-Mandzhiev N.L. (2020). Degradation of lands of the Republic of Kalmykia: problems and ways of their restoration. Arid Ecosystems, 26(2), 63-71.
- Kulik, K.N., Kryuckov, S.N., Malanina, Z.I., & Semenyutina, A.V. (2018). The strategy of protective forestation development in Russian Federation for a period till 2025 year, remade and supplemented. Federal Scientific Center of Agroecology of the Russian Academy of Sciences.
- 9. Konikow, L.F., & Kendy, E. (2005). Groundwater depletion: A global problem. Hydrogeology Journal, 13(1), 317-320. https://doi.org/10.1007/s10040-004-0411-8
- Jones, E., Qadir, M., Van Vliet, M.T.H., Smakhtin, V., & Kang, S. (2019). The state of desalination and brine production: A global outlook. Science of The Total Environment, 657, 1343-1356. https://doi.org/10.1016/j.scitotenv.2018.12.076
- 11. Qadir M., Smakhtin V., Koo-Oshima, S., & G., E. (2022). Unconventional Water Resources. Springer Nature AG, Switzerland. https://doi.org/10.1007/978-3-030-90146-2
- 12. Danilov-Danelyan V.I. (2019). Water Resources of Russia: State, Utilization, Protection, Management, Problems. Economics, Taxes, Pravo, 12(5), 18-31. https://doi:10.26794/1999-849X-2019-12-5-18-31
- 13. Beysens, D., & Milimouk, I. (2000). The Case for Alternative Fresh Water Sources. International Organization for Dew Utilization. Retrieved 10 September 2010.
- Downing, J.A., Prairie, Y.T., Cole, J.J., Duarte, C.M., Tranvik, L.J., Striegl, R.G., McDowell, W.H., & Kortelainen, P., Caraco, N.F. (2006). The global abundance and size distribution of lakes, ponds, and impoundments. Limnology and Oceanography, 51(5), 2388–2397. https://doi:10.4319/lo.2006.51.5.238

- Graham, S., Parkinson, C., & Chahine, M. (2010). The water cycle. NASA Earth Observatory. Available at: https://earthobservatory.nasa.gov/features/Water (accessed 21 April 2020).
- Flossmann, A., Manton, M., Abshaev, A., Bruintjes, R., Murakami, M., Prabhaharan, T., & Yao, Z. (2019). Review of advances in precipitation enhancement research. Bull. Am. Meteorol. Soc. 100, 1465–1480. https://doi.org/10.1175/BAMS-D-18-0160
- 17. Korneev, V.P., Shchukin, G.G., Kim, N.S., Koloskov, B.P. et al. (2019). Artificial regulation of atmospheric precipitation and fog dispersion. Moscow.
- Abshaev, A.M., Flossmann, A., Siems, S.T., Prabhakaran, T., Yao, Z., & Tessendorf, S. (2022). Rain Enhancement Through Cloud Seeding. In M. Qadir et al. (Eds.), Unconventional Water Resources. Springer. http://doi. org/10.1007/978-3-030-90146-2
- Al Hosari, T., Abdulla Al Mandous, Wehbe, Y., Shalaby, A., Al Shamsi, N., Al Naqbi, H., Al Yazeedi, O., Al Mazroui, A., & Farrah, S. (2021). The UAE cloud seeding program: A statistical and physical evaluation. Atmosphere, 12(8), 1013. https://doi.org/10.3390/atmos12081013
- Wehbe, Y., Griffiths, G., Al Mazroui, A., Al Yazeedi, O., & Al Mandous, A. (2023). Rethinking water security in a warming climate: rainfall enhancement as an innovative augmentation technique. NPJ Clim Atmos Sci 6, 171. https://doi.org/10.1038/s41612-023-00503-2
- Fromm, M.D., & Servranckx, R. (2003). Transport of forest fire smoke above the tropopause by supercell convection. Geophys. Res. Lett., 30, 1542. https:// doi:10.1029/2002GL016820
- Fromm, M.D., Bevilacqua, R., Servranckx, R., Rosen, J., Thayer, J., Herman, J., & Larko, D. (2005). Pyro-cumulonimbus injection of smoke to the stratosphere: Observations and impact of a super blowup in northwestern Canada on 3-4 August 1998. J. Geophys. Res., 110, D08205. https:// doi:10.1029/2004JD005350
- 23. Rosenfeld, D., Fromm, M., Trentmann, J., Luderer, G., & Andrea, M.O. (2007). The Chisholm firestorm: Observed microstructure, precipitation and lightning activity of a Pyro-Cb. Atmos. Chem. Phys., 7, 645–659.
- 24. Espy, J.P. (1851). Second and Third Reports on Meteorology to the Secretary of Navy, Washington, 31st Cong., 1st sess. S. Ex. Doc. 30.
- 25. Dessens, H., & Dessens, J. (1964). Exp'eriences avec le meteotronean Centre de Recherches Atmosph'eriques. J. Rech. Atmosph. 1, 158–162.
- Dessens, H. (1965). Pourrons-nous Modifier les Climats? Broch'e 95.
- 27. Vulfson, N.I., & Levin, L.M. (1987). Meteotron as the means of influence on the atmosphere. M.: Gidrometeoizdat.
- 28. "Kuznetsov". Moscow: Publishing House "Stolichnaya Encyclopedia", 5, 124-130.
- Kuznetsov, A.A., & Konopasov, N.G. (2015). The Meteotron. Book No 2. Experiments. Observations. Assessments.
 Registrations. Publishing House of Vladimir State University.
- 30. Kachurin, L.G. (1990). Physical bases of atmospheric processes modification. Leningrad: Hydrometizdat.
- 31. Pomykala, E.S. (1951). Method and Apparatus for making Artificial Rain. U.S. Patent No. 2740663.

- 32. Fuchs, D. (2005). Spain goes hi-tech to beat drought. The Guardian. Retrieved 2007-08-02.
- 33. Duffie, J.A., & Beckman, W.A. (2013). Solar Engineering of Thermal Processes. Fourth Edition.
- Branch, O., Behrendt, A., Gong, Z., Schwitalla, T., & Wulfmeyer, V. (2020). Convection Initiation over the Eastern Arabian Peninsula. Meteorologische Zeitschrift, 29, 67–77. https://doi.org/10.1127/metz/2019/0997
- 35. Oranovsky, V.V. (1994). Atmospheric precipitation induction method. Russian Patent RU 2071243. https://doi.patents.google.com/patent/RU2071243C1/ru
- 36. Brenig, L., Zaady, E., Vigo-Agular, J., Karnieli, A., Fovell, R., Arbel, S., Al Baz, I., & Offer, Z.Y. (2008). Cloud formation and rainfalls induced by artificial solar setting: a weather engineering project for fighting aridity. In Geographical Forum Geographical Studies and Environment Protection Research, 7, 67-82.
- Wulfmeyer V, Behrendt A, Kottmeier C, Corsmeier U, Barthlott C, Craig GC, & Hagen M. (2011). The Convective and Orographically-induced Precipitation Study (COPS): The scientific strategy, the field phase, and research highlights.
 Q. J. R. Meteorol. Soc. 137, 3–30. https://doi:10.1002/qi.752
- 38. Abshaev M.T., Zakinyan R.G., Abshaev A.M., Zakinyan A.R., Ryzhkov R.R., Wehbe, Y., & Al Mandous, A. (2022). Atmospheric conditions favorable for the creation of artificial clouds by a jet saturated with hygroscopic aerosol. Atmospheric Research, 106323. https://doi.org/10.1016/j. atmosres.2022.106323
- Lindsey, D.T., & Fromm, M. (2008). Evidence of the cloud lifetime effect from wildfire-induced thunderstorms. Geophys. Res. Lett., 35, L22809. https:// doi:10.1029/2008GL035680
- 40. Changnon, S.A. (1972). Urban effects on thunderstorm and hailstorm frequencies. Proc. of 2nd Conf. on Biometeorology. Philadelphia, P. 177-184.
- 41. Khemani, L.T., & Ramana-Murty, B.V. (1973). Rainfall Variations in an Urban Industrial Region. J. Appl. Met., 12, 187-194.
- 42. Arizona Board of Regents. (2006). Urban Climate Climate Study and UHI. Arizona State University. Archived from the original on 2007-11-23. Retrieved 2007-08-02.
- 43. Goddard Space Flight Center. (2002). NASA Satellite Confirms Urban Heat Islands Increase Rainfall Around Cities. National Aeronautics and Space Administration. Archived from the original on June 12, 2008.
- 44. Mattes, F.C. (2005). Nuclear power and climate change. Heinrich Böll Foundation.
- Abshaev, M.T., Abshaev, A.M., & Al Mandous, A. (2019). Method of creating artificial clouds and precipitation. Russian Patent RU 2732710. https://doi.patents.google.com/patent/RU2732710C1/ru
- Abshaev, M.T., Abshaev, A.M., Zakinyan, R.G., Zakinyan, A.R., Wehbe, Y., Yousef, L., Farrah, S., & Al Mandous, A. (2020). Investigating the feasibility of artificial convective cloud creation. Atmospheric Research, 243, 104998. https:// doi.org/10.1016/j.atmosres.2020.104998
- Abshaev, M.T., Abshaev, A.M., Aksenov, A.A., Fisher, J.V., Shchelyaev, A.E., & Al Mandous, A. (2023). Study of the Possibility of Stimulating Cloud Convection by Solar Radiation Energy Absorbed in an Artificial Aerosol Layer. Atmosphere, 14, 86. https://doi.org/10.3390/atmos14010086

- 48. Abshaev, M.T., Abshaev, A.M., & Aksenov, A.A. (2022). Simulation of large-scale convective atmospheric flows in FlowVision CFD. In Parallel Computing Technologies. Dubna.
- Abshaev, M.T., Abshaev, A.M., & Al Mandous, A. (2022). Method of creation of artificial clouds and precipitation. Russian Patent RU 2803352. https://doi.patents.google.com/patent/RU2803352C1/ru
- 50. Pavlyuchenko, V.P. (2019). Generation of Artificial Updrafts in the Atmosphere by a Multilevel Facility. Bulletin of the Lebedev Physics Institute, 46(5), 165–169.
- Abshaev, A.M., Abshaev, M.T., & Al Mandous, A. (2020). Method and device for creation of artificial clouds and precipitation. Russian Patent RU 2738479. https://doi.patents.google.com/patent/RU2738479C1/ru
- Abshaev, M.T., Abshaev, A.M., Aksenov, A.A., Fisher, I.V., Shchelyaev, A.E., Al Mandous, A., Wehbe, Y., & El-Khazali, R. (2022). CFD simulation of updrafts initiated by a vertically directed jet fed by the heat of water vapor condensation. Sci. Reports, 12, 9356. https://doi.org/10.1038/s41598-022-13185-2
- Liang, H., Abshaev, M.T., Abshaev, A.M., Huchunaev, B.M., Griffiths, S., & Zou, L. (2019). Water vapor harvesting nanostructures through bioinspired gradient-driven mechanism. Chemical Physics Letters, 728, 167-173. https://doi.org/10.1016/j.cplett.2019.05.008
- 54. Tai, Y., Liang, H., El Hadri, N., Abshaev, A., Huchunaev, B., Griffiths, S., Jouaid, M., & Zou, L. (2017). Core/Shell Microstructure Induced Synergistic Effect for Efficient Water-Droplet Formation and Cloud-Seeding Application. ACS Nano. https://pubs.acs.org/doi/10.1021/acsnano.7b06114
- Tverskoy P.N. (1962). Course of meteorology. Leningrad: Hydrometizdat.
- Abshaev, A.M., Abshaev, M.T., Barekova, M.V., & Malkarova, A.M. (2014). Manual on Hail Suppression. Nalchik, Printing House.
- 57. Abramovich, G.N. (1984). The Theory of Turbulent Jets. Moscow: Scientific Press.
- Abshaev M.T., Abshaev A.M., Aksenov A.A., Fisher J.V., Shchelyaev A.E., & Al Mandous, A. (2023). Results of Field Experiments for the Creation of Artificial Updrafts and Clouds. Atmosphere, 14, 136. https://doi.org/10.3390/ atmos14010136
- Drofa, A.S., Ivanov, V.N., Rosenfeld D., & Shilin, A.G. (2010). Studying an effect of salt powder seeding used for precipitation enhancement from convective clouds. Atmosph. Chem. Phys., 10, 8011–8023. https://doi:10.5194/acp-10-8011-2010

- Haoran, L., Abshaev, M.T., Abshaev, A.M., Huchunaev, B.M., Griffiths, S., & Zou, L. (2019). Water vapor harvesting nanostructures through bioinspired gradient-driven mechanism. Chem. Phys. Lett. 728, 167-173. https://doi. org/10.1016/j.cplett.2019.05.008.
- 61. Wood, B.K. (2002). Propulsion for the 21ST Century RS-68. American Institute of Aeronautics and Astronautics.
- 62. Danilchenko, V.P. (2018). History of development of Russian liquid-propellant rocket-space engines PJSC.
- 63. Belyaeva, M.V., Drofa, A.S., & Ivanov, V.N. (2013). Efficiency of stimulating precipitation from convective clouds using salt powders. Izv. Atmos. Ocean. Phys. 49, 154–161. https://doi.org/10.1134/S0001433813010039
- 64. Landau, L. D. (1944). About one exact solution of the Navier-Stokes equations. Reports of the USSR Academy of Sciences, 43(7), 299-301.
- Abshaev, M.T., Zakinyan, R.G., Abshaev, A.M., Al-Owaidi, Q.S.K., Zakinyan, A.R., Wehbe, Y., Yousef, L., Farrah, S., & Al Mandous, A. (2019). Influence of Atmosphere Near Surface Layer Properties on Development of Cloud Convection. Atmosphere, 10, 131. https://doi.org/10.3390/atmos10030131
- Abshaev, M.T., Abshaev, A.M., Malkarova, A.M., & Mizieva J.Y. (2009). Radar estimation of water content in Cb clouds. Izv. Atmos. Ocean. Phys. 45, 731–736. https://doi.org/10.1134/S0001433809060061
- 67. Aladin, N.V., & Plotnikov, I.S. (1995). Drying up of the Aral Sea and possible ways of rehabilitation and conservation of its northern part. Proc. of the Zoological Institute of Russian Academy of Sci., 262, 3-16.
- 68. Atkinson, B. W. (1975). The Mechanical Effect of an Urban Area on Convective Precipitation. Occasional Paper 3, Dept. of Geography, Queen Mary College, Univ. of London.
- 69. Benech B. (1976). Experimental study of an artificial convective plume initiated from the ground. J. Appl. Meteorology, 15(2), 127-137.
- 70. FlowVision. (n.d.). User's Guide 3.12.02. Company TESIS. Retrieved from https://flowvision.ru/webhelp/fvru 31201
- 71. Mie, G. (2008). Beitrage zur optic truber medien speziel kolloidaler metalosungen. Ann. Phys., 25, 377-422. https://doi:10.1002/andp.19083300302
- 72. New UNICEF-WHO Report. (2023, July 6).
- 73. Wikipedia. (n.d.). Top ten largest (non-polar) deserts. Archived from original on 2021-01-26.
- 74. Tereshchenko, A.G. (2015). Deliquescence: Hygroscopicity of Water-Soluble Crystalline Solids. J Pharm Sci., 104(11), 3639-3652. https://doi:10.1002/jps.24589

Copyright: © 2025 by the contributors and Crystal Scientific Publishers. This work is licensed under the Creative Commons Attribution International License.